



Physics-based Device Simulation

C. Jungemann

Institut für Theoretische Elektrotechnik RWTH Aachen University 52056 Aachen



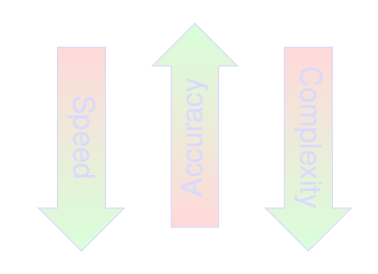


Outline

- Motivation
- Pros & Cons
- Semiclassical transport
- Results
- Conclusions

Simulation hierarchy

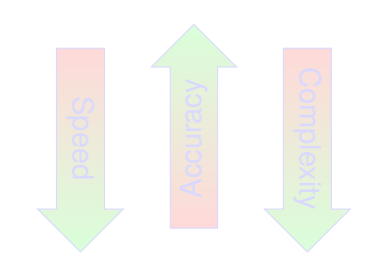
- Quantum transport
- Semiclassical transport
- ► TCAE
- Compact models



- Complex band structures
- Detailed scattering models
- Only material-dependent parameters
- DC, AC and noise analysis
- No adjustable parameters in the RF noise model

Simulation hierarchy

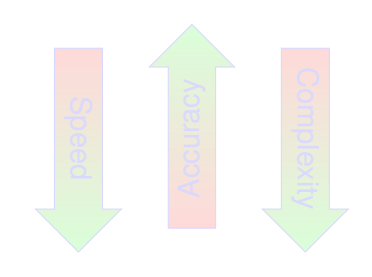
- Quantum transport
- Semiclassical transport
- ► TCAD
- Compact models



- Complex band structures
- Detailed scattering models
- Only material-dependent parameters
- DC, AC and noise analysis
- No adjustable parameters in the RF noise model

Simulation hierarchy

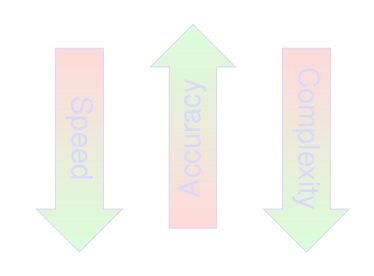
- Quantum transport
- Semiclassical transport
- ► TCAE
- Compact models



- Complex band structures
- Detailed scattering models
- Only material-dependent parameters
- DC, AC and noise analysis
- No adjustable parameters in the RF noise model

Simulation hierarchy

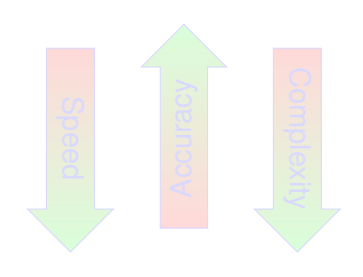
- Quantum transport
- Semiclassical transport
- TCAD
- Compact models



- Complex band structures
- Detailed scattering models
- Only material-dependent parameters
- DC, AC and noise analysis
- No adjustable parameters in the RF noise model

Simulation hierarchy

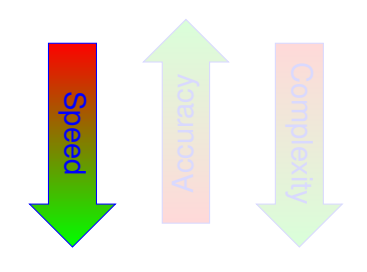
- Quantum transport
- Semiclassical transport
- TCAD
- Compact models



- Complex band structures
- Detailed scattering models
- Only material-dependent parameters
- DC, AC and noise analysis
- No adjustable parameters in the RF noise model

Simulation hierarchy

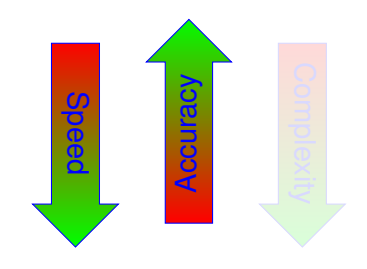
- Quantum transport
- Semiclassical transport
- TCAD
- Compact models



- Complex band structures
- Detailed scattering models
- Only material-dependent parameters
- DC, AC and noise analysis
- No adjustable parameters in the RF noise model

Simulation hierarchy

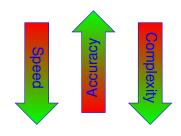
- Quantum transport
- Semiclassical transport
- TCAD
- Compact models



- Complex band structures
- Detailed scattering models
- Only material-dependent parameters
- DC, AC and noise analysis
- No adjustable parameters in the RF noise model

Simulation hierarchy

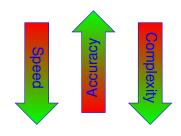
- Quantum transport
- Semiclassical transport
- TCAD
- Compact models



- Complex band structures
- Detailed scattering models
- Only material-dependent parameters
- DC, AC and noise analysis
- No adjustable parameters in the RF noise model

Simulation hierarchy

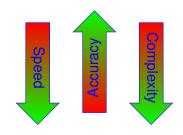
- Quantum transport
- Semiclassical transport
- TCAD
- Compact models



- Complex band structures
- Detailed scattering models
- Only material-dependent parameters
- DC, AC and noise analysis
- No adjustable parameters in the RF noise model

Simulation hierarchy

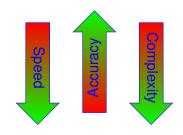
- Quantum transport
- Semiclassical transport
- TCAD
- Compact models



- Complex band structures
- Detailed scattering models
- Only material-dependent parameters
- DC, AC and noise analysis
- No adjustable parameters in the RF noise model

Simulation hierarchy

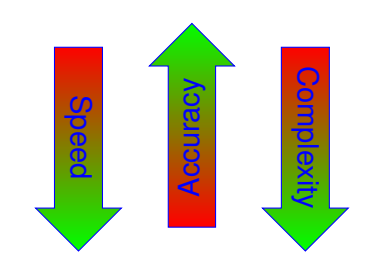
- Quantum transport
- Semiclassical transport
- TCAD
- Compact models



- Complex band structures
- Detailed scattering models
- Only material-dependent parameters
- DC, AC and noise analysis
- No adjustable parameters in the RF noise model

Simulation hierarchy

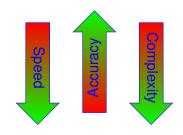
- Quantum transport
- Semiclassical transport
- TCAD
- Compact models



- Complex band structures
- Detailed scattering models
- Only material-dependent parameters
- DC, AC and noise analysis
- No adjustable parameters in the RF noise model

Simulation hierarchy

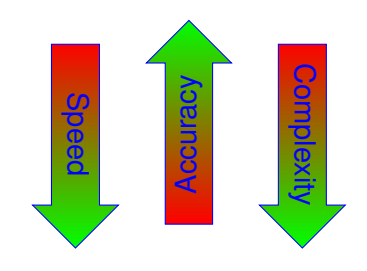
- Quantum transport
- Semiclassical transport
- TCAD
- Compact models



- Complex band structures
- Detailed scattering models
- Only material-dependent parameters
- DC, AC and noise analysis
- No adjustable parameters in the RF noise model

Simulation hierarchy

- Quantum transport
- Semiclassical transport
- TCAD
- Compact models



- Complex band structures
- Detailed scattering models
- Only material-dependent parameters
- DC, AC and noise analysis
- No adjustable parameters in the RF noise model

- Realistic device structure
- Microscopic, accurate physics (Boltzmann equation)
- Detailed physics
- Consistent modeling of transport and noise
- Numerically challenging
- Very slow (a CPU day per bias point for a 2D device)
- ► Limited device detail (2D, only few parasitics)
- Only as good as the models

Pros & Cons

- Realistic device structure
- Microscopic, accurate physics (Boltzmann equation)
- Detailed physics
- Consistent modeling of transport and noise
- Numerically challenging
- Very slow (a CPU day per bias point for a 2D device)
- Limited device detail (2D, only few parasitics)
- Only as good as the models

Pros & Cons

- Realistic device structure
- Microscopic, accurate physics (Boltzmann equation)
- Detailed physics
- Consistent modeling of transport and noise
- Numerically challenging
- Very slow (a CPU day per bias point for a 2D device)
- Limited device detail (2D, only few parasitics)
- Only as good as the models

Pros & Cons

- Realistic device structure
- Microscopic, accurate physics (Boltzmann equation)
- Detailed physics
- Consistent modeling of transport and noise
- Numerically challenging
- Very slow (a CPU day per bias point for a 2D device)
- Limited device detail (2D, only few parasitics)
- Only as good as the models

- Realistic device structure
- Microscopic, accurate physics (Boltzmann equation)
- Detailed physics
- Consistent modeling of transport and noise
- Numerically challenging
- Very slow (a CPU day per bias point for a 2D device
- Limited device detail (2D, only few parasitics)
- Only as good as the models

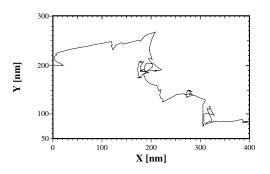
- Realistic device structure
- Microscopic, accurate physics (Boltzmann equation)
- Detailed physics
- Consistent modeling of transport and noise
- Numerically challenging
- Very slow (a CPU day per bias point for a 2D device)
- Limited device detail (2D, only few parasitics)
- Only as good as the models

- Realistic device structure
- Microscopic, accurate physics (Boltzmann equation)
- Detailed physics
- Consistent modeling of transport and noise
- Numerically challenging
- Very slow (a CPU day per bias point for a 2D device)
- Limited device detail (2D, only few parasitics)
- Only as good as the models

- Realistic device structure
- Microscopic, accurate physics (Boltzmann equation)
- Detailed physics
- Consistent modeling of transport and noise
- Numerically challenging
- Very slow (a CPU day per bias point for a 2D device)
- Limited device detail (2D, only few parasitics)
- Only as good as the models

- Realistic device structure
- Microscopic, accurate physics (Boltzmann equation)
- Detailed physics
- Consistent modeling of transport and noise
- Numerically challenging
- Very slow (a CPU day per bias point for a 2D device)
- Limited device detail (2D, only few parasitics)
- Only as good as the models

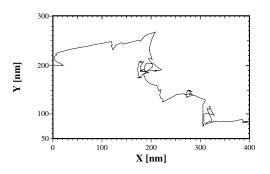
Path of an electron in a semiconductor



Newton's equations of motion

$$\frac{\mathrm{d}\vec{p}}{\mathrm{d}t} = \vec{F} \; , \qquad \frac{\mathrm{d}\vec{r}}{\mathrm{d}t} = i$$

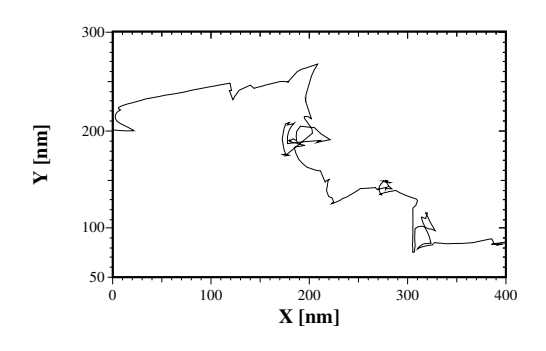
Path of an electron in a semiconductor



Newton's equations of motion

$$\frac{\mathrm{d}\vec{p}}{\mathrm{d}t} = \vec{F} \; , \qquad \frac{\mathrm{d}\vec{r}}{\mathrm{d}t} = i$$

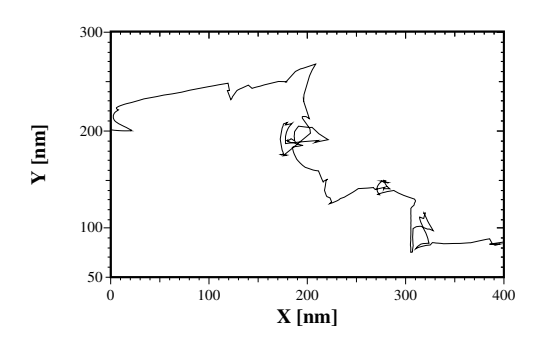
Path of an electron in a semiconductor



Newton's equations of motion

$$\frac{\mathrm{d}\vec{p}}{\mathrm{d}t} = \vec{F} \; , \qquad \frac{\mathrm{d}\vec{r}}{\mathrm{d}t} = \vec{v}$$

Path of an electron in a semiconductor



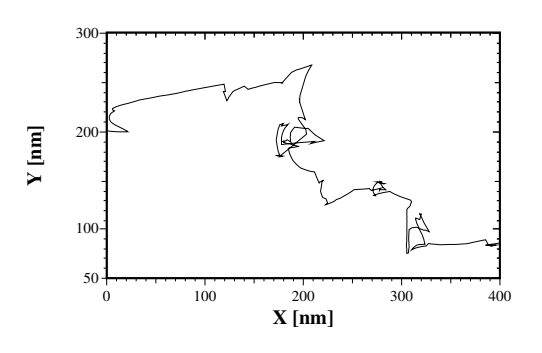
Newton's equations of motion

$$\frac{\mathrm{d}\vec{p}}{\mathrm{d}t} = \vec{F} \; , \qquad \frac{\mathrm{d}\vec{r}}{\mathrm{d}t} = \vec{v}$$

Two first order ODEs

Two initial conditions (position, momentum)

Path of an electron in a semiconductor



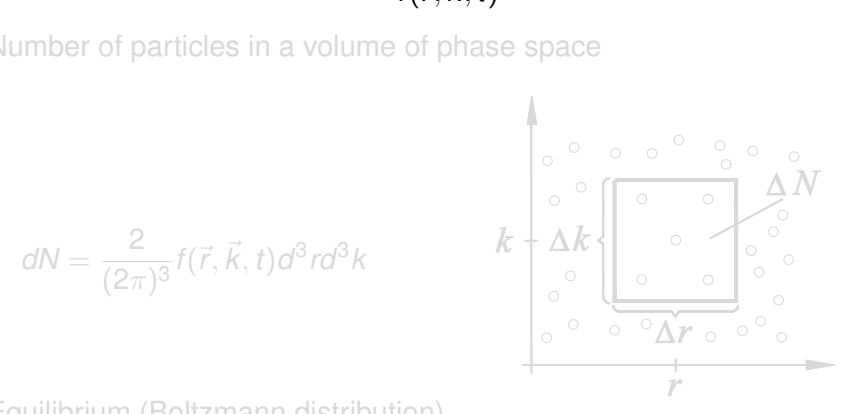
Newton's equations of motion

$$\frac{\mathrm{d}\vec{p}}{\mathrm{d}t} = \vec{F} \; , \qquad \frac{\mathrm{d}\vec{r}}{\mathrm{d}t} = \vec{v}$$

Particle ensemble described by a distribution function $(\vec{p} = \hbar \vec{k})$

$$f(\vec{r}, \vec{k}, t)$$

$$dN = \frac{2}{(2\pi)^3} f(\vec{r}, \vec{k}, t) d^3 r d^3 k$$



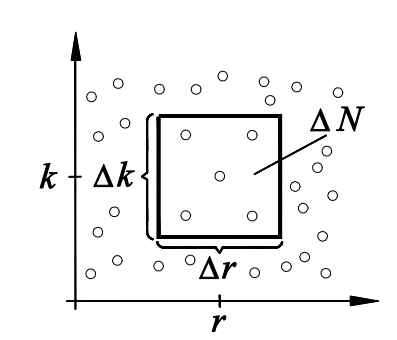
$$f_0 = c \exp\left(-\frac{\varepsilon(\vec{r}, \vec{k})}{kT}\right)$$

Particle ensemble described by a distribution function $(\vec{p} = \hbar \vec{k})$

$$f(\vec{r}, \vec{k}, t)$$

Number of particles in a volume of phase space

$$dN = rac{2}{(2\pi)^3} f(\vec{r}, \vec{k}, t) d^3 r d^3 k$$



Equilibrium (Boltzmann distribution)

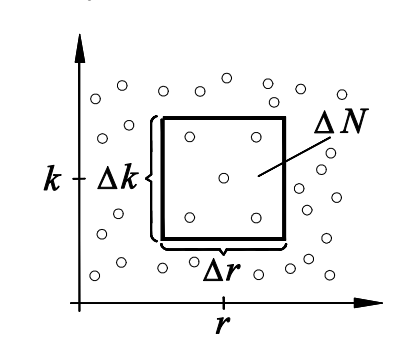
$$f_0 = c \exp\left(-\frac{\varepsilon(\vec{r}, \vec{k})}{kT}\right)$$

Particle ensemble described by a distribution function $(\vec{p} = \hbar \vec{k})$

$$f(\vec{r}, \vec{k}, t)$$

Number of particles in a volume of phase space

$$dN=rac{2}{(2\pi)^3}f(\vec{r},\vec{k},t)d^3rd^3k$$



Equilibrium (Boltzmann distribution)

$$f_0 = c \exp\left(-\frac{\varepsilon(\vec{r}, \vec{k})}{kT}\right)$$

Boltzmann Transport Equation

$$\begin{split} \frac{\partial f\left(\vec{r},\vec{k},t\right)}{\partial t} - \frac{q}{\hbar} \vec{E}(\vec{r}) \cdot \nabla_{\vec{k}} f\left(\vec{r},\vec{k},t\right) + \vec{v}\left(\vec{k}\right) \cdot \nabla_{\vec{r}} f\left(\vec{r},\vec{k},t\right) = \\ \frac{\Omega_{\text{sys}}}{(2\pi)^3} \int W\left(\vec{r},\vec{k}|\vec{k}'\right) f\left(\vec{r},\vec{k}',t\right) - W\left(\vec{r},\vec{k}'|\vec{k}\right) f\left(\vec{r},\vec{k},t\right) d^3k' \end{split}$$

Integro-differential equation

Direct discretization of the 6D phase space is not possible

Spherical Harmonics Expansion solver (SHE) for the BTE (Bologna group, Maryland group et al.)

Boltzmann Transport Equation

$$\begin{split} \frac{\partial f\left(\vec{r},\vec{k},t\right)}{\partial t} - \frac{q}{\hbar} \vec{E}(\vec{r}) \cdot \nabla_{\vec{k}} f\left(\vec{r},\vec{k},t\right) + \vec{v}\left(\vec{k}\right) \cdot \nabla_{\vec{r}} f\left(\vec{r},\vec{k},t\right) = \\ \frac{\Omega_{\text{sys}}}{(2\pi)^3} \int W\left(\vec{r},\vec{k}|\vec{k}'\right) f\left(\vec{r},\vec{k}',t\right) - W\left(\vec{r},\vec{k}'|\vec{k}\right) f\left(\vec{r},\vec{k},t\right) d^3k' \end{split}$$

Integro-differential equation

Direct discretization of the 6D phase space is not possible

Spherical Harmonics Expansion solver (SHE) for the BTE (Bologna group, Maryland group et al.)

Boltzmann Transport Equation

$$\begin{split} \frac{\partial f\left(\vec{r},\vec{k},t\right)}{\partial t} - \frac{q}{\hbar} \vec{E}(\vec{r}) \cdot \nabla_{\vec{k}} f\left(\vec{r},\vec{k},t\right) + \vec{v}\left(\vec{k}\right) \cdot \nabla_{\vec{r}} f\left(\vec{r},\vec{k},t\right) = \\ \frac{\Omega_{\text{sys}}}{(2\pi)^3} \int W\left(\vec{r},\vec{k}|\vec{k}'\right) f\left(\vec{r},\vec{k}',t\right) - W\left(\vec{r},\vec{k}'|\vec{k}\right) f\left(\vec{r},\vec{k},t\right) d^3k' \end{split}$$

Integro-differential equation

Direct discretization of the 6D phase space is not possible

Spherical Harmonics Expansion solver (SHE) for the BTE (Bologna group, Maryland group et al.)

Boltzmann Transport Equation

$$\begin{split} \frac{\partial f\left(\vec{r},\vec{k},t\right)}{\partial t} - \frac{q}{\hbar} \vec{E}(\vec{r}) \cdot \nabla_{\vec{k}} f\left(\vec{r},\vec{k},t\right) + \vec{v}\left(\vec{k}\right) \cdot \nabla_{\vec{r}} f\left(\vec{r},\vec{k},t\right) = \\ \frac{\Omega_{sys}}{(2\pi)^3} \int W\left(\vec{r},\vec{k}|\vec{k}'\right) f\left(\vec{r},\vec{k}',t\right) - W\left(\vec{r},\vec{k}'|\vec{k}\right) f\left(\vec{r},\vec{k},t\right) d^3k' \end{split}$$

Integro-differential equation

Direct discretization of the 6D phase space is not possible

Spherical Harmonics Expansion solver (SHE) for the BTE (Bologna group, Maryland group et al.)

Spherical coordinates for k-space

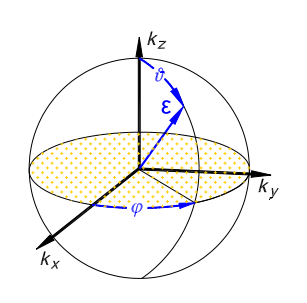
$$(k_{\mathsf{X}},k_{\mathsf{y}},k_{\mathsf{z}})$$
 \rightarrow (k,ϑ,φ) \rightarrow $(\varepsilon,\vartheta,\varphi)$

$$Y_{0,0} = \frac{1}{\sqrt{4\pi}}$$

$$Y_{1,-1} = \sqrt{\frac{3}{4\pi}} \sin \vartheta \sin \varphi$$

$$Y_{1,0} = \sqrt{\frac{3}{4\pi}} \cos \vartheta$$

$$Y_{1,1} = \sqrt{\frac{3}{4\pi}} \sin \vartheta \cos \varphi$$



$$\oint Y_{l,m}(\vartheta,\varphi)Y_{l',m'}(\vartheta,\varphi)d\Omega = \delta_{l,l'}\delta_{m,m'}\;, \qquad d\Omega = \sin\vartheta d\vartheta darphi$$

Spherical coordinates for k-space

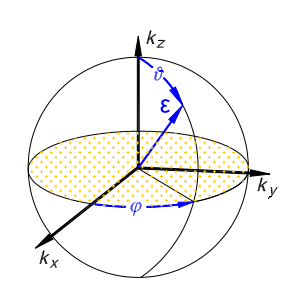
$$(k_x, k_y, k_z) \rightarrow (k, \vartheta, \varphi) \rightarrow (\varepsilon, \vartheta, \varphi)$$

$$Y_{0,0} = \frac{1}{\sqrt{4\pi}}$$

$$Y_{1,-1} = \sqrt{\frac{3}{4\pi}} \sin \vartheta \sin \varphi$$

$$Y_{1,0} = \sqrt{\frac{3}{4\pi}} \cos \vartheta$$

$$Y_{1,1} = \sqrt{\frac{3}{4\pi}} \sin \vartheta \cos \varphi$$



$$\oint Y_{l,m}(\vartheta,\varphi)Y_{l',m'}(\vartheta,\varphi)d\Omega = \delta_{l,l'}\delta_{m,m'}\;, \qquad d\Omega = \sin\vartheta d\vartheta darphi$$

Spherical coordinates for k-space

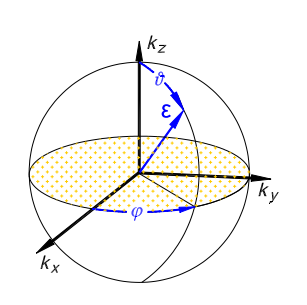
$$(k_x, k_y, k_z) \rightarrow (k, \vartheta, \varphi) \rightarrow (\varepsilon, \vartheta, \varphi)$$

$$Y_{0,0} = \frac{1}{\sqrt{4\pi}}$$

$$Y_{1,-1} = \sqrt{\frac{3}{4\pi}} \sin \vartheta \sin \varphi$$

$$Y_{1,0} = \sqrt{\frac{3}{4\pi}} \cos \vartheta$$

$$Y_{1,1} = \sqrt{\frac{3}{4\pi}} \sin \vartheta \cos \varphi$$



$$\oint Y_{l,m}(\vartheta,\varphi)Y_{l',m'}(\vartheta,\varphi)d\Omega = \delta_{l,l'}\delta_{m,m'}\;, \qquad d\Omega = \sin\vartheta d\vartheta darphi$$

Spherical coordinates for k-space

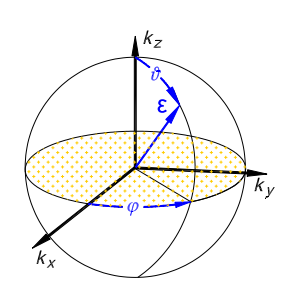
$$(k_x, k_y, k_z) \rightarrow (k, \vartheta, \varphi) \rightarrow (\varepsilon, \vartheta, \varphi)$$

$$Y_{0,0} = \frac{1}{\sqrt{4\pi}}$$

$$Y_{1,-1} = \sqrt{\frac{3}{4\pi}} \sin \vartheta \sin \varphi$$

$$Y_{1,0} = \sqrt{\frac{3}{4\pi}} \cos \vartheta$$

$$Y_{1,1} = \sqrt{\frac{3}{4\pi}} \sin \vartheta \cos \varphi$$

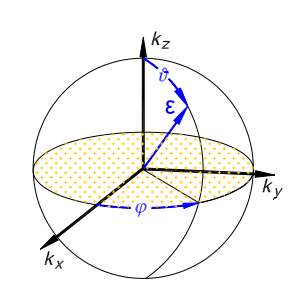


$$\oint Y_{l,m}(\vartheta,\varphi)Y_{l',m'}(\vartheta,\varphi)d\Omega = \delta_{l,l'}\delta_{m,m'}\;, \qquad d\Omega = \sin\vartheta d\vartheta d\varphi$$

Spherical coordinates for k-space

$$(k_x, k_y, k_z) \rightarrow (k, \vartheta, \varphi) \rightarrow (\varepsilon, \vartheta, \varphi)$$

$$Y_{0,0} = rac{1}{\sqrt{4\pi}}$$
 $Y_{1,-1} = \sqrt{rac{3}{4\pi}} \sin artheta \sin arphi$
 $Y_{1,0} = \sqrt{rac{3}{4\pi}} \cos artheta$
 $Y_{1,1} = \sqrt{rac{3}{4\pi}} \sin artheta \cos arphi$



$$\oint Y_{l,m}(\vartheta,\varphi)Y_{l',m'}(\vartheta,\varphi)d\Omega = \delta_{l,l'}\delta_{m,m'}, \qquad d\Omega = \sin\vartheta d\vartheta d\varphi$$

Spherical harmonics expansion of the distribution function

$$g_{l,m}(\vec{r},\varepsilon,t) = \frac{1}{(2\pi)^3} \int \delta\left(\varepsilon - \varepsilon(\vec{k})\right) Y_{l,m}(\vartheta,\varphi) f(\vec{r},\vec{k},t) d^3k$$

$$g(\vec{r}, \vec{k}, t) = g(\vec{r}, \varepsilon, \vartheta, \varphi, t) \approx \sum_{l=0}^{l_{\max}} \sum_{m=-l}^{m=l} g_{l,m}(\vec{r}, \varepsilon, t) Y_{l,m}(\vartheta, \varphi)$$

Electron density

$$n(\vec{r},t) = \frac{2}{(2\pi)^3} \int f(\vec{r},\vec{k},t) d^3k = 2\sqrt{4\pi} \int_0^\infty g_{0,0}(\vec{r},\varepsilon,t) d\varepsilon$$

Electron current density (spherical bands

$$\vec{j}(\vec{r},t) = 2\sqrt{\frac{4\pi}{3}} \int_0^\infty v(\varepsilon) \begin{pmatrix} g_{1,1}(\vec{r},\varepsilon,t) \\ g_{1,-1}(\vec{r},\varepsilon,t) \\ g_{1,0}(\vec{r},\varepsilon,t) \end{pmatrix} d\varepsilon$$

Spherical harmonics expansion of the distribution function

$$g_{l,m}(\vec{r},\varepsilon,t) = \frac{1}{(2\pi)^3} \int \delta\left(\varepsilon - \varepsilon(\vec{k})\right) Y_{l,m}(\vartheta,\varphi) f(\vec{r},\vec{k},t) d^3k$$

$$g(\vec{r}, \vec{k}, t) = g(\vec{r}, \varepsilon, \vartheta, \varphi, t) \approx \sum_{l=0}^{l_{\text{max}}} \sum_{m=-l}^{m=l} g_{l,m}(\vec{r}, \varepsilon, t) Y_{l,m}(\vartheta, \varphi)$$

Electron density

$$n(\vec{r},t) = \frac{2}{(2\pi)^3} \int f(\vec{r},\vec{k},t) d^3k = 2\sqrt{4\pi} \int_0^\infty g_{0,0}(\vec{r},\varepsilon,t) d\varepsilon$$

Electron current density (spherical bands

$$\vec{j}(\vec{r},t) = 2\sqrt{\frac{4\pi}{3}} \int_0^\infty v(\varepsilon) \begin{pmatrix} g_{1,1}(\vec{r},\varepsilon,t) \\ g_{1,-1}(\vec{r},\varepsilon,t) \\ g_{1,0}(\vec{r},\varepsilon,t) \end{pmatrix} d\varepsilon$$

Spherical harmonics expansion of the distribution function

$$g_{l,m}(\vec{r},\varepsilon,t) = \frac{1}{(2\pi)^3} \int \delta\left(\varepsilon - \varepsilon(\vec{k})\right) Y_{l,m}(\vartheta,\varphi) f(\vec{r},\vec{k},t) d^3k$$

$$g(\vec{r}, \vec{k}, t) = g(\vec{r}, \varepsilon, \vartheta, \varphi, t) \approx \sum_{l=0}^{l_{\max}} \sum_{m=-l}^{m=l} g_{l,m}(\vec{r}, \varepsilon, t) Y_{l,m}(\vartheta, \varphi)$$

Electron density

$$n(\vec{r},t) = \frac{2}{(2\pi)^3} \int f(\vec{r},\vec{k},t) d^3k = 2\sqrt{4\pi} \int_0^\infty g_{0,0}(\vec{r},\varepsilon,t) d\varepsilon$$

Electron current density (spherical bands

$$\vec{j}(\vec{r},t) = 2\sqrt{\frac{4\pi}{3}} \int_0^\infty v(\varepsilon) \begin{pmatrix} g_{1,1}(\vec{r},\varepsilon,t) \\ g_{1,-1}(\vec{r},\varepsilon,t) \\ g_{1,0}(\vec{r},\varepsilon,t) \end{pmatrix} d\varepsilon$$

Spherical harmonics expansion of the distribution function

$$g_{l,m}(\vec{r},\varepsilon,t) = \frac{1}{(2\pi)^3} \int \delta\left(\varepsilon - \varepsilon(\vec{k})\right) Y_{l,m}(\vartheta,\varphi) f(\vec{r},\vec{k},t) d^3k$$

$$g(\vec{r},\vec{k},t) = g(\vec{r},\varepsilon,\vartheta,\varphi,t) \approx \sum_{l=1}^{l_{\text{max}}} \sum_{m=l}^{m=l} g_{l,m}(\vec{r},\varepsilon,t) Y_{l,m}(\vartheta,\varphi)$$

Electron density

$$n(\vec{r},t) = \frac{2}{(2\pi)^3} \int f(\vec{r},\vec{k},t) d^3k = 2\sqrt{4\pi} \int_0^\infty g_{0,0}(\vec{r},\varepsilon,t) d\varepsilon$$

Electron current density (spherical bands)

$$\vec{j}(\vec{r},t) = 2\sqrt{\frac{4\pi}{3}} \int_0^\infty v(\varepsilon) \begin{pmatrix} g_{1,1}(\vec{r},\varepsilon,t) \\ g_{1,-1}(\vec{r},\varepsilon,t) \\ g_{1,0}(\vec{r},\varepsilon,t) \end{pmatrix} d\varepsilon$$

Spherical harmonics expansion of the Boltzmann equation

$$\frac{1}{(2\pi)^3}\int \delta\left(\varepsilon-\varepsilon(\vec{k})\right)\,Y_{l,m}(\vartheta,\varphi)\,\{\mathsf{BE}\}\,d^3k$$

yields balance equations over energy/real space

$$\frac{\partial g_{l,m}}{\partial t} - q\vec{E} \cdot \frac{\partial j_{l,m}}{\partial \varepsilon} + \nabla_{\vec{l}} \cdot \vec{j}_{l,m} - \Gamma_{l,m} = W_{l,m}\{g\}$$

with

$$\vec{j}_{l,m}(\vec{r},arepsilon,t) = v(arepsilon) \sum_{l',m'} \vec{a}_{l,m,l',m'} g_{l'.m'}(\vec{r},arepsilon,t)$$

Spherical harmonics expansion of the Boltzmann equation

$$\frac{1}{(2\pi)^3}\int \delta\left(\varepsilon-\varepsilon(\vec{k})\right)\,Y_{l,m}(\vartheta,\varphi)\,\{\mathsf{BE}\}\,d^3k$$

yields balance equations over energy/real space

$$\frac{\partial g_{l,m}}{\partial t} - q\vec{E} \cdot \frac{\partial \vec{j}_{l,m}}{\partial \varepsilon} + \nabla_{\vec{r}} \cdot \vec{j}_{l,m} - \Gamma_{l,m} = W_{l,m}\{g\}$$

with

$$\vec{j}_{l,m}(\vec{r},\varepsilon,t) = v(\varepsilon) \sum_{l',m'} \vec{a}_{l,m,l',m'} g_{l',m'}(\vec{r},\varepsilon,t)$$

Spherical harmonics expansion of the Boltzmann equation

$$\frac{1}{(2\pi)^3}\int \delta\left(\varepsilon-\varepsilon(\vec{k})\right)\,Y_{l,m}(\vartheta,\varphi)\,\{{\sf BE}\}\,d^3k$$

yields balance equations over energy/real space

$$\frac{\partial g_{l,m}}{\partial t} - q\vec{E} \cdot \frac{\partial \vec{j}_{l,m}}{\partial \varepsilon} + \nabla_{\vec{r}} \cdot \vec{j}_{l,m} - \Gamma_{l,m} = W_{l,m}\{g\}$$

with

$$\vec{j}_{l,m}(\vec{r},\varepsilon,t) = v(\varepsilon) \sum_{l',m'} \vec{a}_{l,m,l',m'} g_{l'.m'}(\vec{r},\varepsilon,t)$$

Spherical harmonics expansion of the Boltzmann equation

$$\frac{1}{(2\pi)^3}\int \delta\left(\varepsilon-\varepsilon(\vec{k})\right)\,Y_{l,m}(\vartheta,\varphi)\,\{\mathsf{BE}\}\,d^3k$$

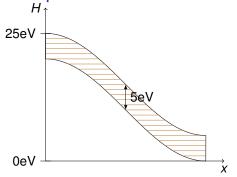
yields balance equations over energy/real space

$$\frac{\partial g_{l,m}}{\partial t} - q\vec{E} \cdot \frac{\partial \vec{j}_{l,m}}{\partial \varepsilon} + \nabla_{\vec{r}} \cdot \vec{j}_{l,m} - \Gamma_{l,m} = W_{l,m}\{g\}$$

with

$$\vec{j}_{l,m}(\vec{r},\varepsilon,t) = v(\varepsilon) \sum_{l',m'} \vec{a}_{l,m,l',m'} g_{l'.m'}(\vec{r},\varepsilon,t)$$

H-transform

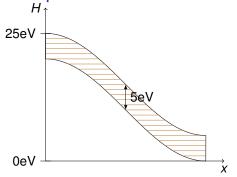


$$H(\vec{r}, \vec{k}) = \varepsilon(\vec{k}) - q\Psi(\vec{r}) \quad \Rightarrow \quad g'(\vec{r}, H, t) = g(\vec{r}, \varepsilon, t)$$

Cancels the energy derivative for the stationary state

$$-g\vec{E}\cdot\frac{\partial\vec{j'}_{l,m}}{\partial z}+\nabla_{\vec{r}}\cdot\vec{j'}_{l,m}-\Gamma'_{l,m}=W_{l,m}\{g'\}$$

H-transform

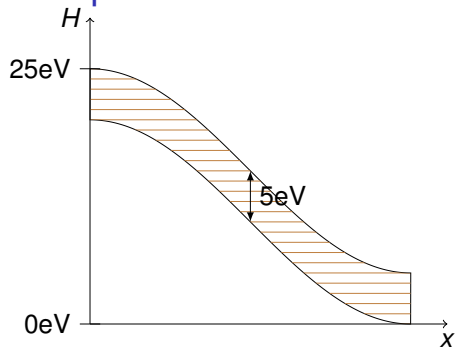


$$H\left(\vec{r},\vec{k}\right) = \varepsilon\left(\vec{k}\right) - q\Psi\left(\vec{r}\right) \quad \Rightarrow \quad g'(\vec{r},H,t) = g(\vec{r},\varepsilon,t)$$

Cancels the energy derivative for the stationary state

$$-g\vec{E}\cdot\frac{\partial\vec{j'}_{l,m}}{\partial\varepsilon}+\nabla_{\vec{r}}\cdot\vec{j'}_{l,m}-\Gamma'_{l,m}=W_{l,m}\{g'\}$$

H-transform

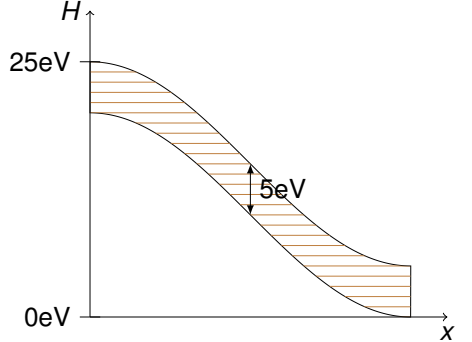


$$H\left(\vec{r},\vec{k}\right) = \varepsilon\left(\vec{k}\right) - q\Psi\left(\vec{r}\right) \quad \Rightarrow \quad g'(\vec{r},H,t) = g(\vec{r},\varepsilon,t)$$

Cancels the energy derivative for the stationary state

$$-q\vec{E}\cdot\frac{\partial\vec{j'}_{l,m}}{\partial\varepsilon}+\nabla_{\vec{r}}\cdot\vec{j'}_{l,m}-\Gamma'_{l,m}=W_{l,m}\{g'\}$$

H-transform



$$H\left(\vec{r},\vec{k}\right) = \varepsilon\left(\vec{k}\right) - q\Psi\left(\vec{r}\right) \quad \Rightarrow \quad g'(\vec{r},H,t) = g(\vec{r},\varepsilon,t)$$

Cancels the energy derivative for the stationary state

$$-g\vec{E}\cdot\frac{\partial\vec{j'}_{l,m}}{\partial\varepsilon}+\nabla_{\vec{r}}\cdot\vec{j'}_{l,m}-\Gamma'_{l,m}=W_{l,m}\{g'\}$$

- H-transform
- Maximum Entropy Dissipation Scheme
- Dimensional splitting
- Box Integration (exact particle number conservation)
- First order expansion has property N
- Newton-Raphson method to solve BE and PE self-consistently

- H-transform
- Maximum Entropy Dissipation Scheme
- Dimensional splitting
- Box Integration (exact particle number conservation)
- First order expansion has property M
- Newton-Raphson method to solve BE and PE self-consistently

- H-transform
- Maximum Entropy Dissipation Scheme
- Dimensional splitting
- Box Integration (exact particle number conservation)
- First order expansion has property M
- Newton-Raphson method to solve BE and PE self-consistently

- H-transform
- Maximum Entropy Dissipation Scheme
- Dimensional splitting
- Box Integration (exact particle number conservation)
- First order expansion has property M
- Newton-Raphson method to solve BE and PE self-consistently

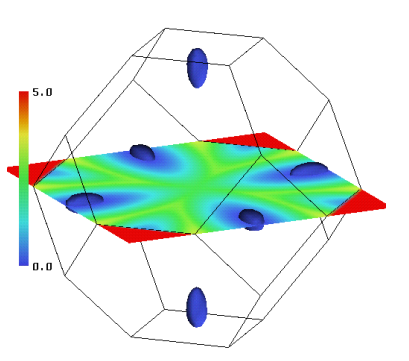
- H-transform
- Maximum Entropy Dissipation Scheme
- Dimensional splitting
- Box Integration (exact particle number conservation)
- First order expansion has property M
- Newton-Raphson method to solve BE and PE self-consistently

- H-transform
- Maximum Entropy Dissipation Scheme
- Dimensional splitting
- Box Integration (exact particle number conservation)
- First order expansion has property M
- Newton-Raphson method to solve BE and PE self-consistently

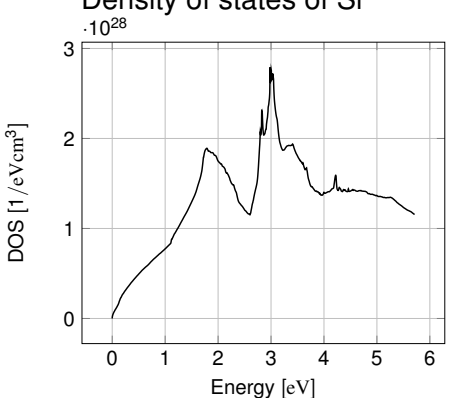
- H-transform
- Maximum Entropy Dissipation Scheme
- Dimensional splitting
- Box Integration (exact particle number conservation)
- First order expansion has property M
- Newton-Raphson method to solve BE and PE self-consistently

Complex band structure effects



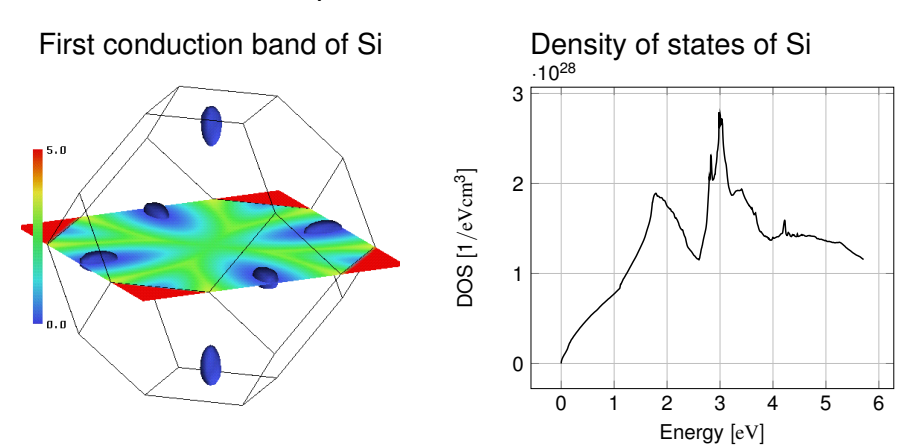


Density of states of Si



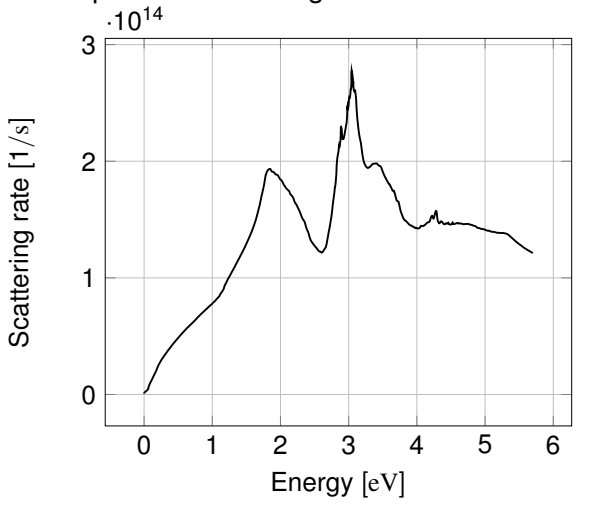
Calculated by the nonlocal empirical pseudopotential method

Complex band structure effects

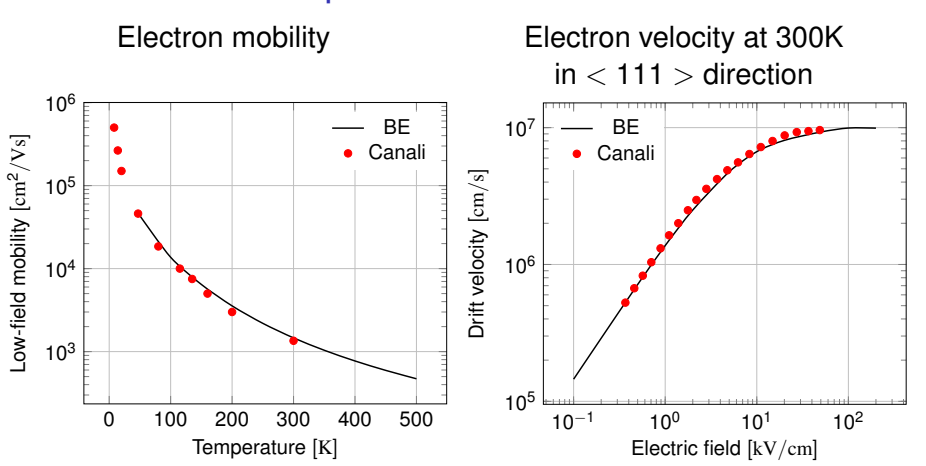


Calculated by the nonlocal empirical pseudopotential method Only DOS and v^2 are required for SHE

Electron-phonon scattering rate of silicon at 300K

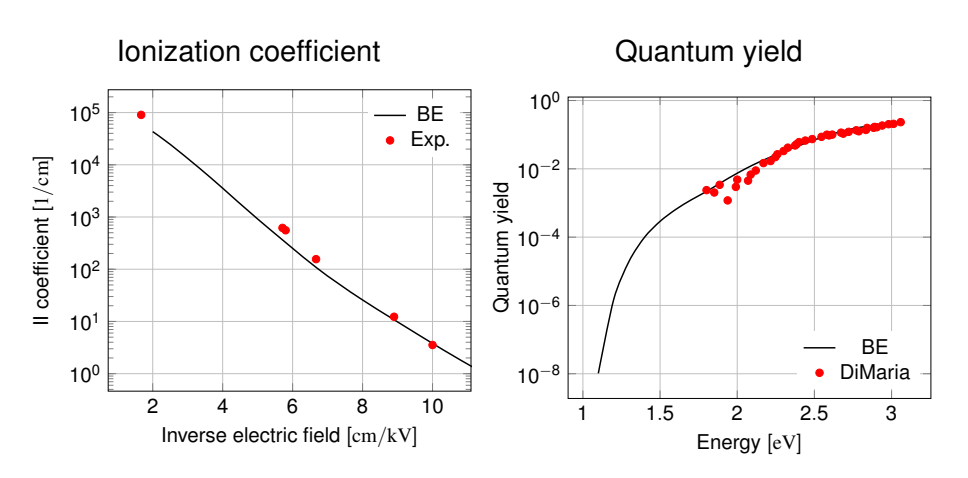


All parameters determined by theory or basic experiments



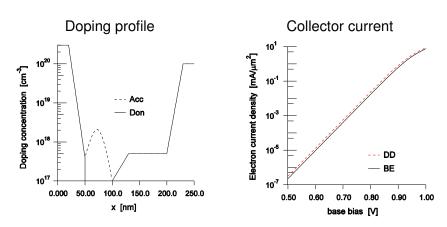
Good agreement between simulation and experiment for silicon

Impact ionization



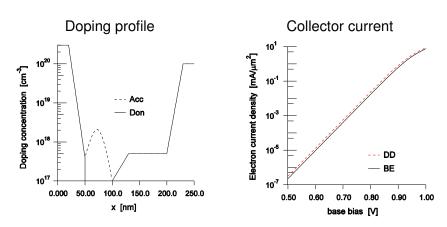
Good agreement between simulation and experiment for silicon

Results



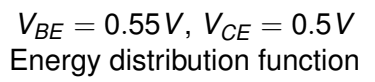
SHE can handle high doping concentrations without problems

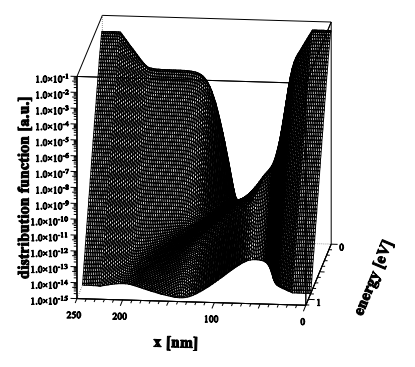
SHE can handle small currents without problems

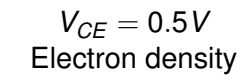


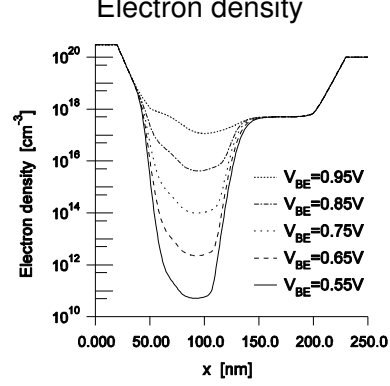
SHE can handle high doping concentrations without problems

SHE can handle small currents without problems





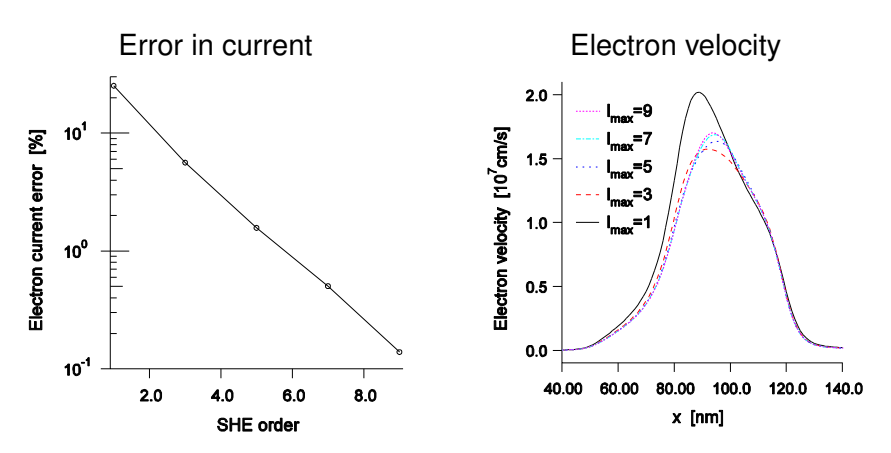




SHE can handle huge variations in the density without problems

Bipolar transistor

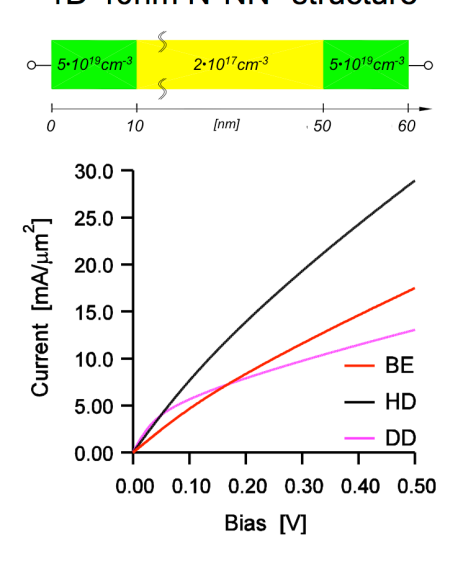
Dependence on the maximum order of SHE $V_{BE} = 0.85 V$, $V_{CE} = 0.5 V$



Transport in nanometric devices requires at least 5th order SHE

N⁺NN⁺ structure

1D 40nm N⁺NN⁺ structure



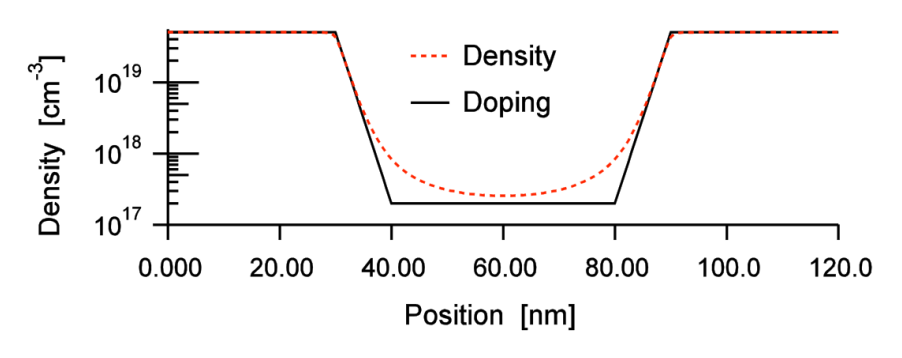
 Macroscopic models (DD, HD) fail for strong nonequilibrium due to

Ballistic transport!

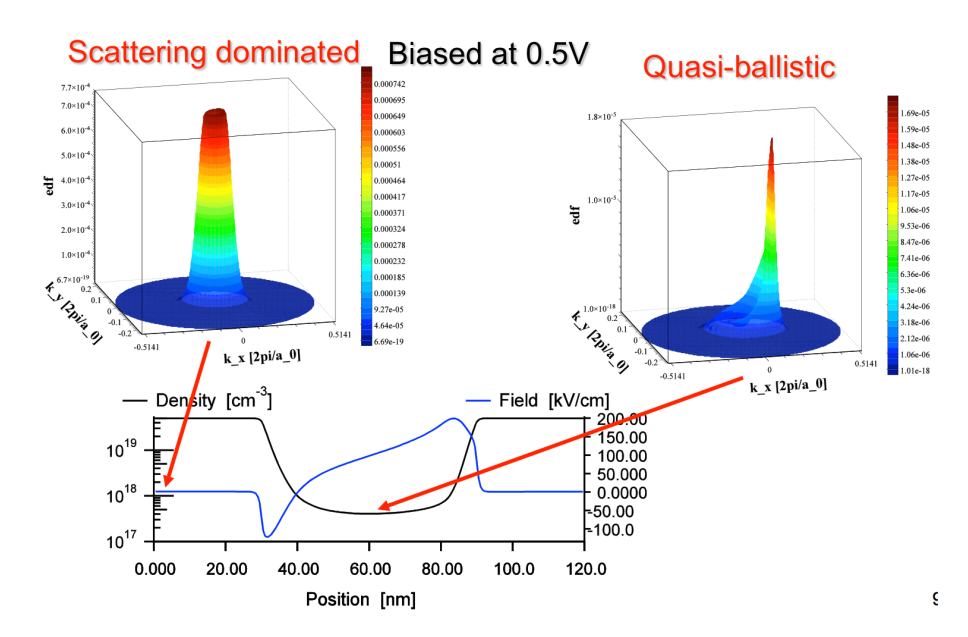
 Macroscopic models also fail near equilibrium in nanometric devices!

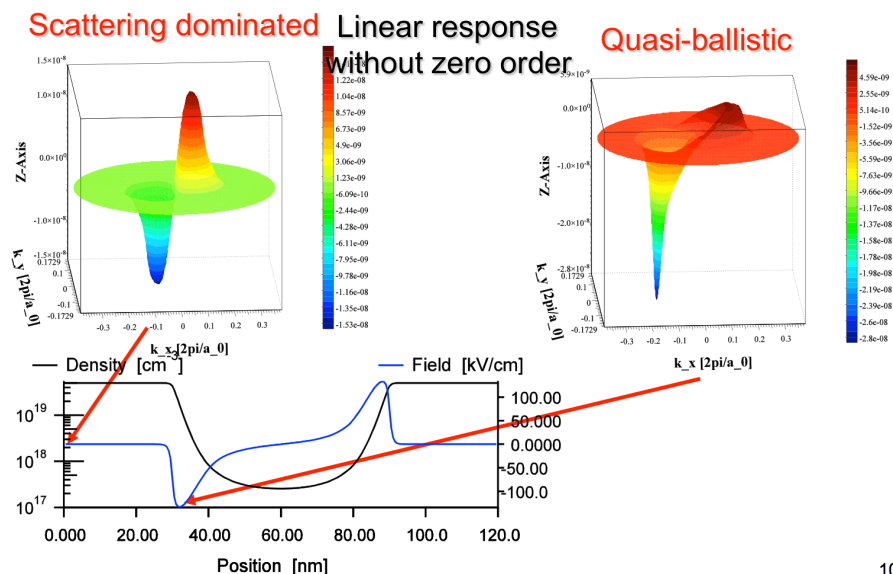
Why?

1D 40nm silicon N⁺NN⁺ structure

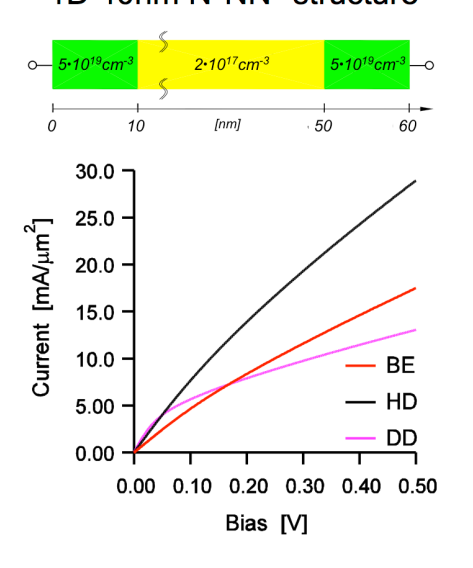


Transport is in x-direction





1D 40nm N⁺NN⁺ structure

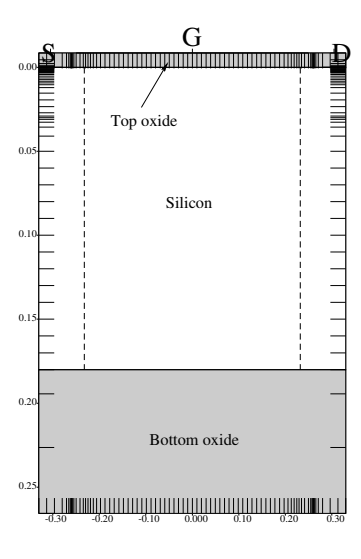


 Macroscopic models (DD, HD) fail for strong nonequilibrium due to

Ballistic transport!

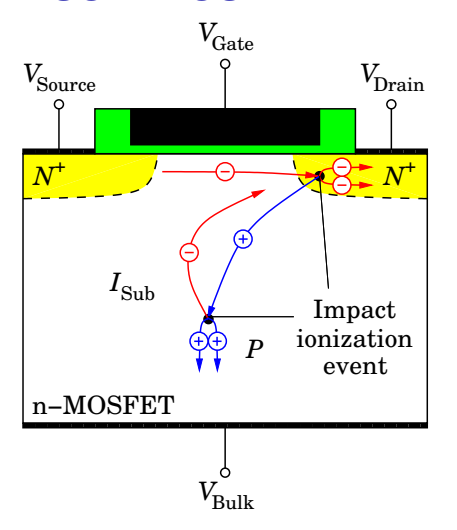
 Macroscopic models also fail near equilibrium in nanometric devices!

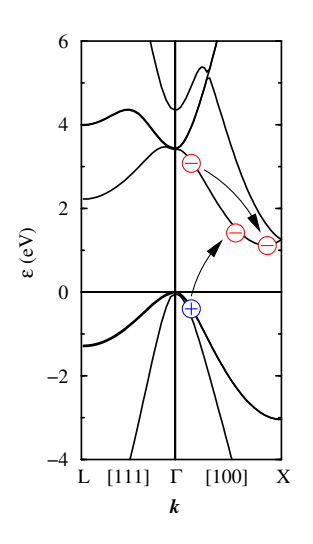
Why?



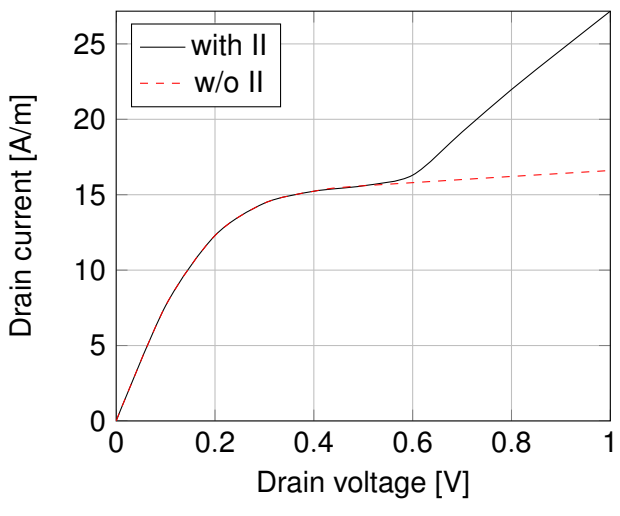
Partially depleted SOI NMOSFET

PDSOI NMOSFET



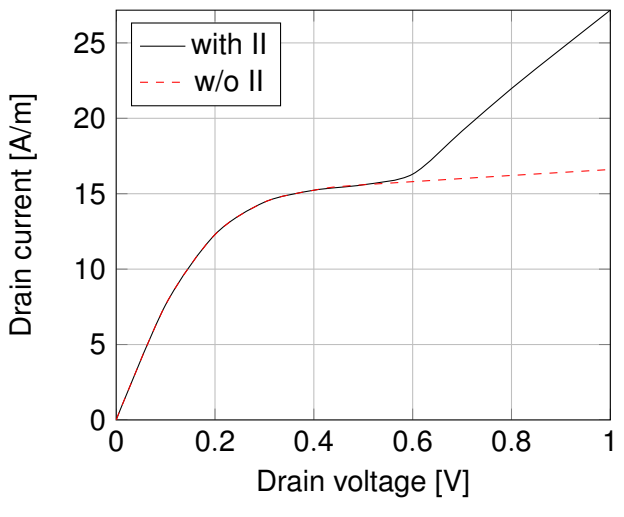


Every impact ionization event generates a secondary electron/hole pair

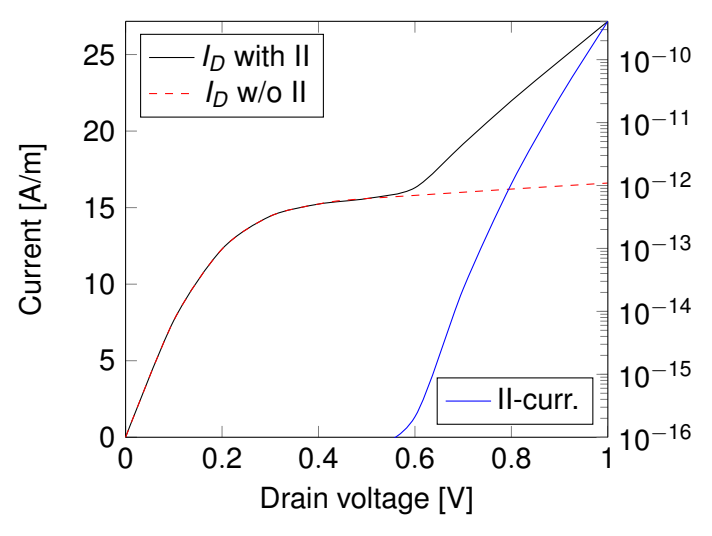


Kink effect due to impact ionization (II) ($V_{\text{gate}} = 1.0 V$)

Exact stationary solutions



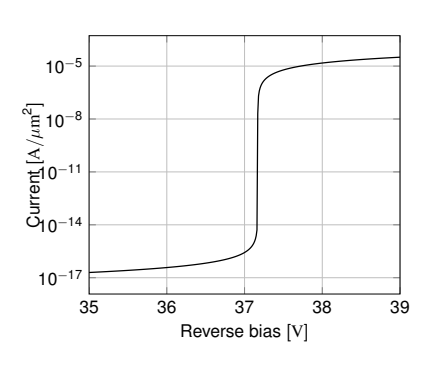
Kink effect due to impact ionization (II) ($V_{\rm gate} = 1.0\,V$) Exact stationary solutions

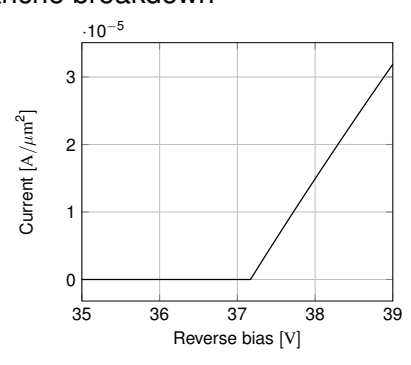


About 17 orders of magnitude difference in currents at kink

pn Junction

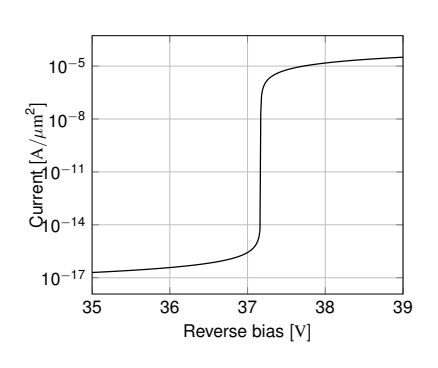
Simulation of avalanche breakdown

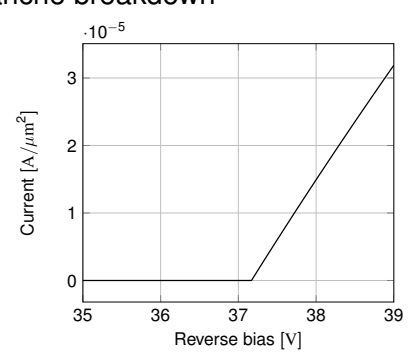




Extremely steep increase of current with voltage ($20\mu V/dec$)

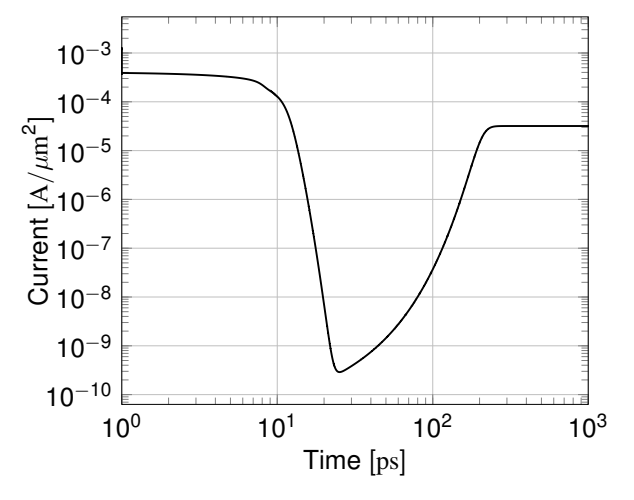
Simulation of avalanche breakdown





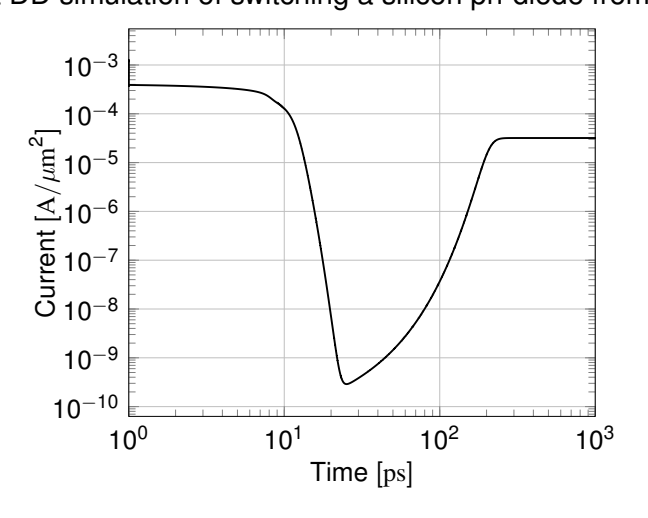
Extremely steep increase of current with voltage (20 μ V/dec)

Transient DD simulation of switching a silicon pn-diode from 0 to -39V



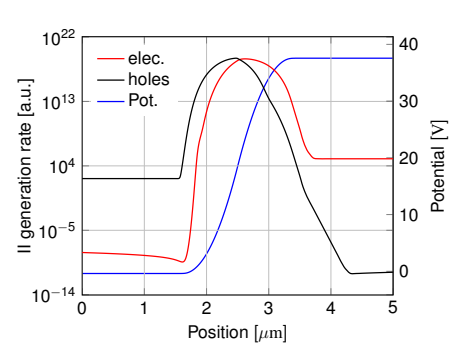
Avalanche breakdown is slow!

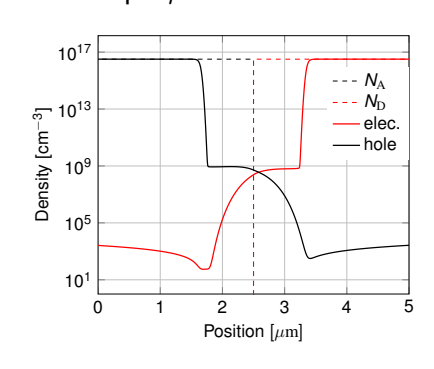
Transient DD simulation of switching a silicon pn-diode from 0 to -39V



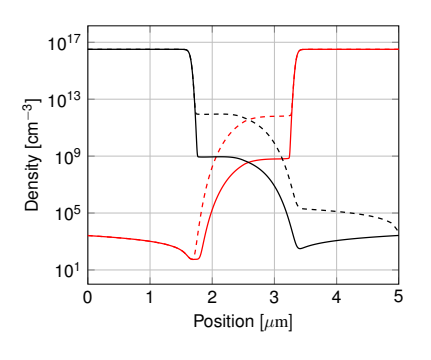
Avalanche breakdown is slow!

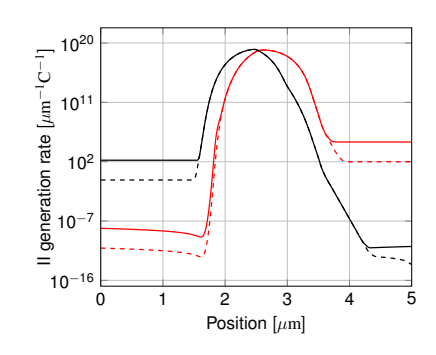
Simulation for 37.172V and $10pA/\mu m^2$





II generation increases number of particles in the space charge region

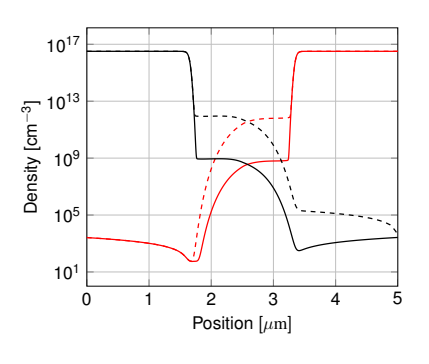


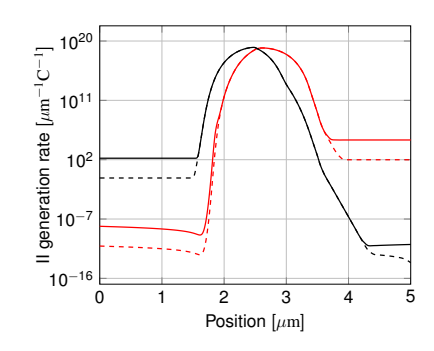


Particle density in the space charge region increases 1000 times

Relevant II generation rate scales with current

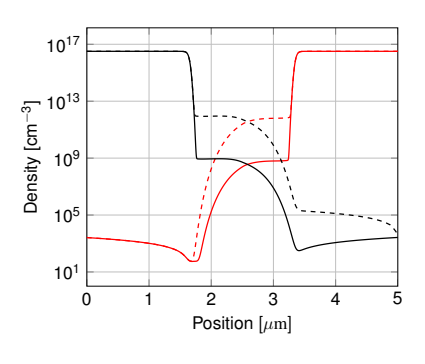
Hot electron/hole effects scale with current

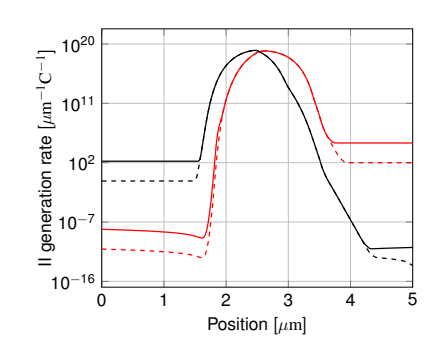




Particle density in the space charge region increases 1000 times

Relevant II generation rate scales with current Hot electron/hole effects scale with current



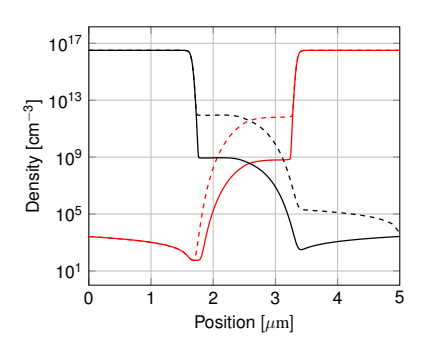


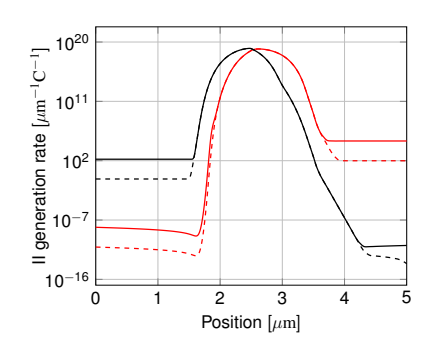
37

Particle density in the space charge region increases 1000 times

Relevant II generation rate scales with current

Hot electron/hole effects scale with current



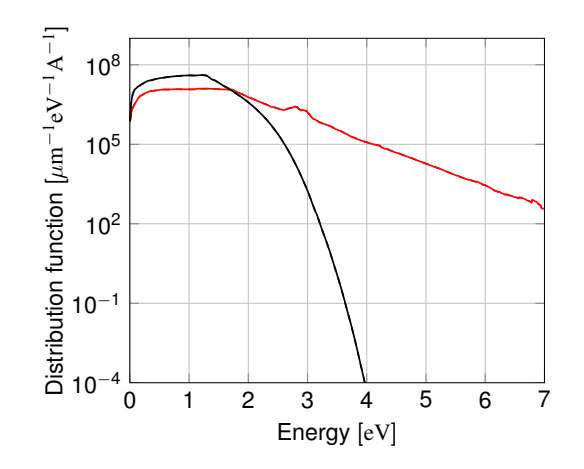


Particle density in the space charge region increases 1000 times

Relevant II generation rate scales with current

Hot electron/hole effects scale with current

Scaled electron/hole distribution function in the middle of the pn junction

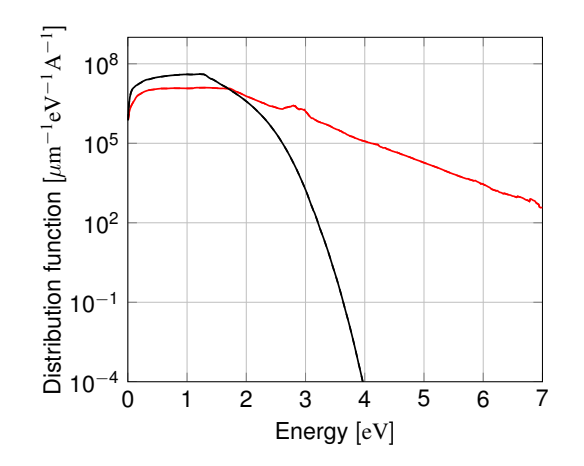


Hot electron/hole effects scale with current

pn Junction

Increase of current by a factor of 1000 (dashed lines)

Scaled electron/hole distribution function in the middle of the pn junction

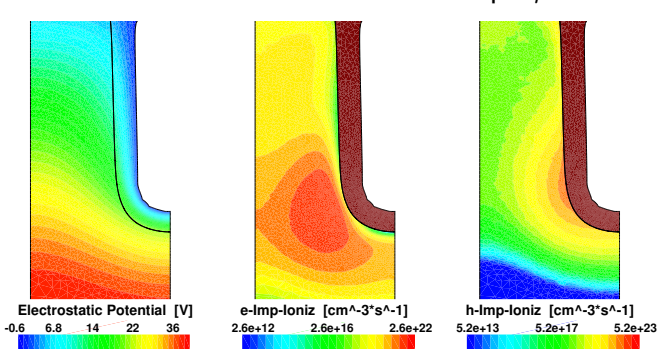


Hot electron/hole effects scale with current

Vertical power transistor

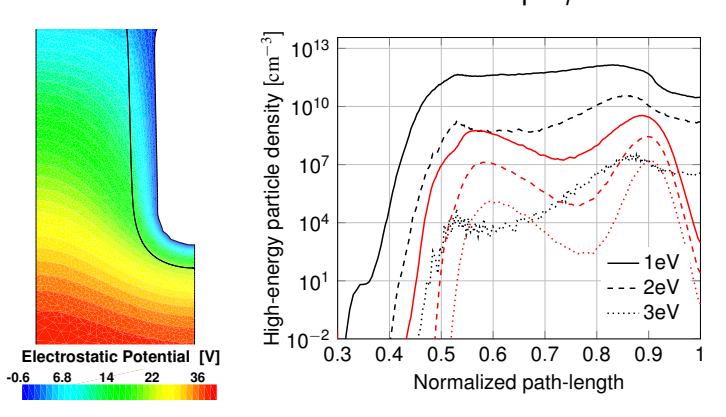
Avalanche breakdown of a power transistor

BE simulation for 35.83V and $10pA/\mu m^2$



45 · 10⁶ variables, 2 CPU hours

BE simulation for 35.83V and $10pA/\mu m^2$

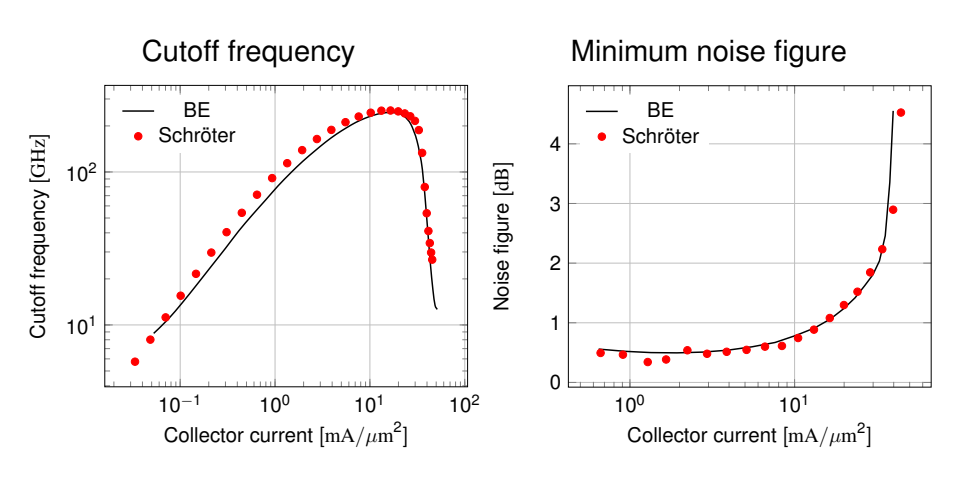


Injection of electrons and holes into the oxide can be calculated

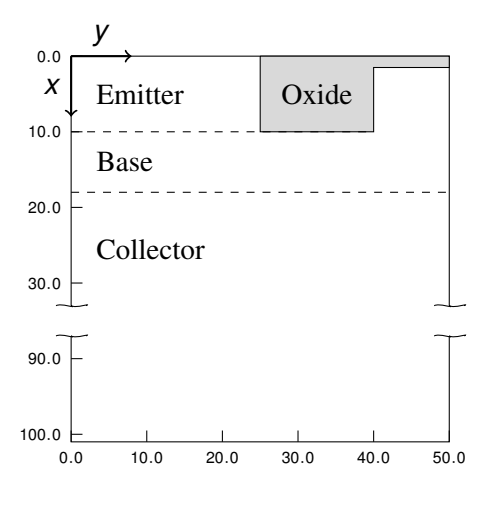
Structure, DC and AC behavior of the npn THz SiGe HBT

Comparison with experiments

Comparison for an ST-Microelectronics SiGe HBT at 10GHz and $V_{\rm CE} = 1.2 \rm V$

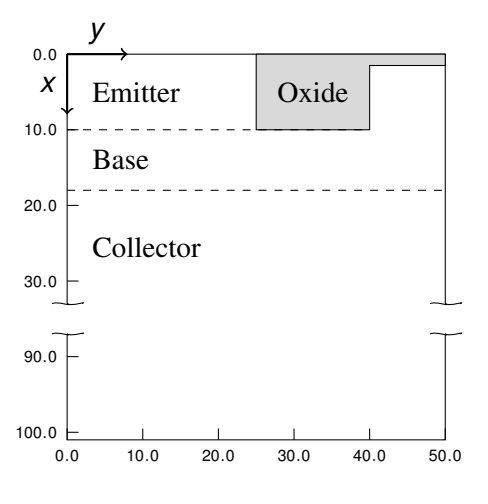


Good agreement between simulation and measurement



Emitter-window width: 2 × 25nm

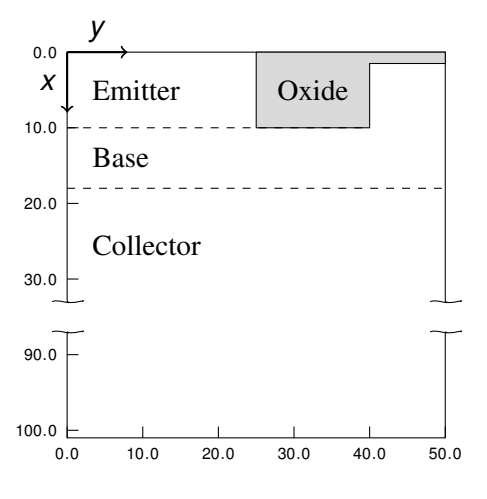
- ▶ 149 nodes in x-direction
- ▶ 20 nodes in *y*-direction
- ► 5th order SHE expansion (21 spherical harmonics)
- ► Up to 1.42 · 10⁸ unknown variables (spacing in energy is 5.17meV and number of energy grid points depends on bias)
- Over 200 GB of memory required (for AC)
- ▶ Up to 10⁵ CPU-seconds for a DC point



Emitter-window width: 2 × 25nm

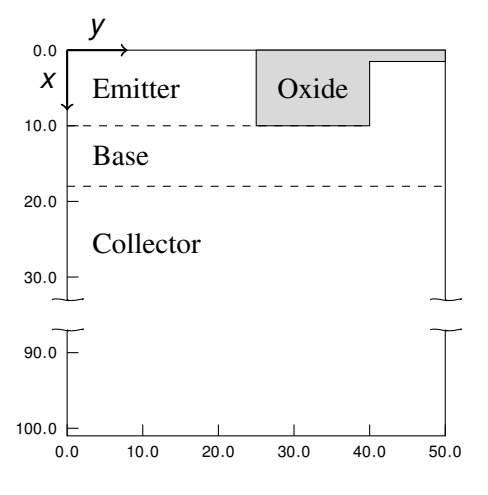
▶ 149 nodes in x-direction

- ▶ 20 nodes in y-direction
- ► 5th order SHE expansion (21 spherical harmonics)
- ► Up to 1.42 · 10⁸ unknown variables (spacing in energy is 5.17meV and number of energy grid points depends on bias)
- Over 200 GB of memory required (for AC)
- ▶ Up to 10⁵ CPU-seconds for a DC point



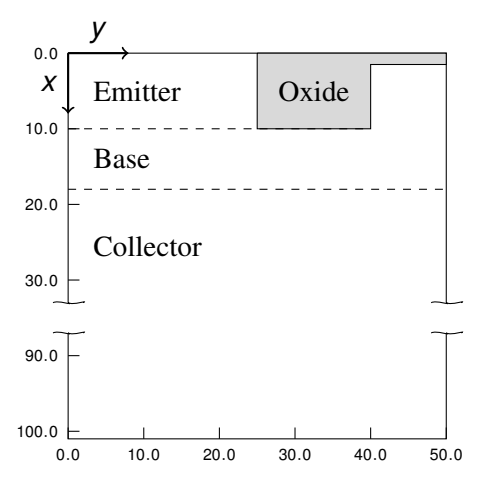
Emitter-window width: 2 × 25nm

- ▶ 149 nodes in x-direction
- ▶ 20 nodes in *y*-direction
- ► 5th order SHE expansion (21 spherical harmonics)
- ► Up to 1.42 · 10⁸ unknown variables (spacing in energy is 5.17meV and number of energy grid points depends on bias)
- Over 200 GB of memory required (for AC)
- ▶ Up to 10⁵ CPU-seconds for a DC point



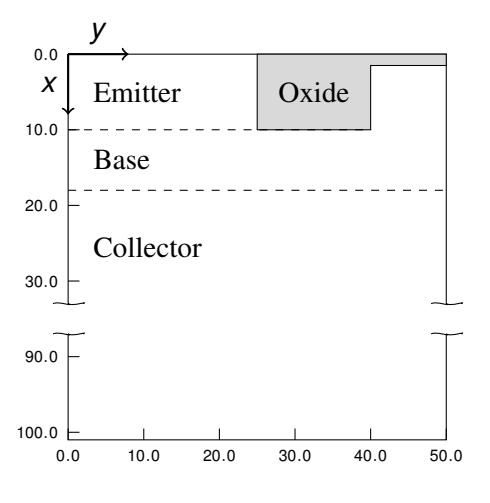
Emitter-window width: 2 × 25nm

- ▶ 149 nodes in x-direction
- ▶ 20 nodes in *y*-direction
- 5th order SHE expansion (21 spherical harmonics)
- ► Up to 1.42 · 10⁸ unknown variables (spacing in energy is 5.17meV and number of energy grid points depends on bias)
- Over 200 GB of memory required (for AC)
- ▶ Up to 10⁵ CPU-seconds for a DC point



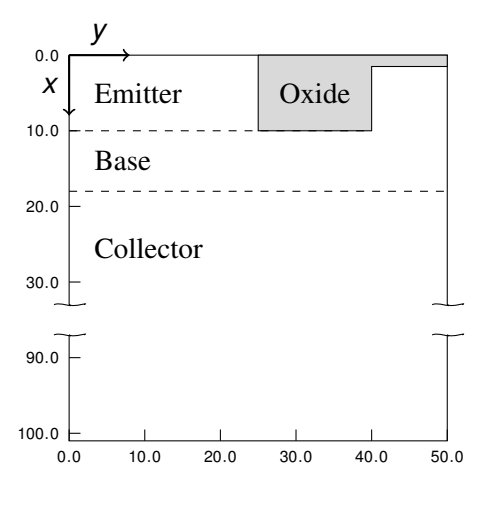
Emitter-window width: 2 × 25nm

- ▶ 149 nodes in x-direction
- ▶ 20 nodes in *y*-direction
- 5th order SHE expansion (21 spherical harmonics)
- ▶ Up to 1.42 · 10⁸ unknown variables (spacing in energy is 5.17meV and number of energy grid points depends on bias)
- Over 200 GB of memory required (for AC)
- ▶ Up to 10⁵ CPU-seconds for a DC point



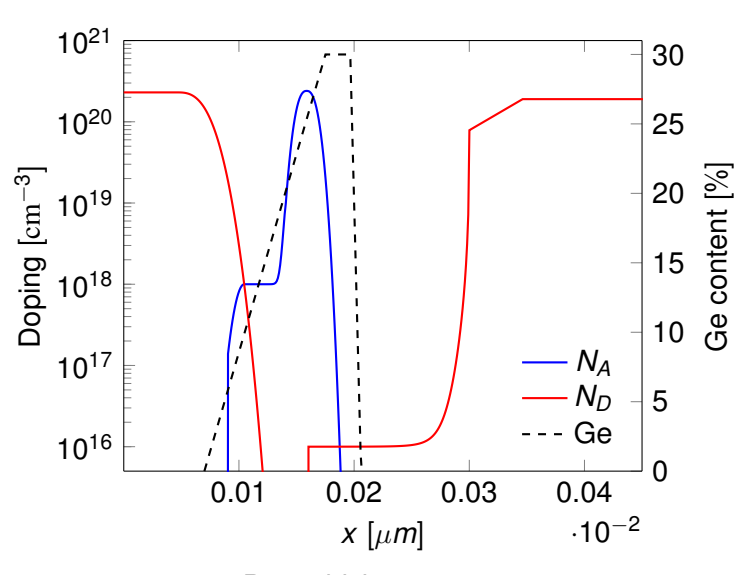
Emitter-window width: 2 × 25nm

- ▶ 149 nodes in x-direction
- ▶ 20 nodes in *y*-direction
- 5th order SHE expansion (21 spherical harmonics)
- ▶ Up to 1.42 · 10⁸ unknown variables (spacing in energy is 5.17meV and number of energy grid points depends on bias)
- Over 200 GB of memory required (for AC)
- ▶ Up to 10⁵ CPU-seconds for a DC point

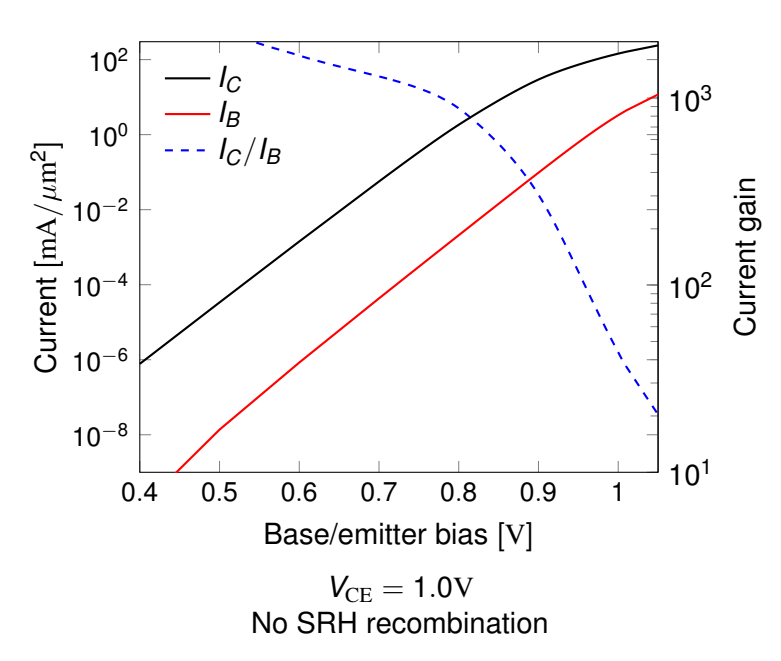


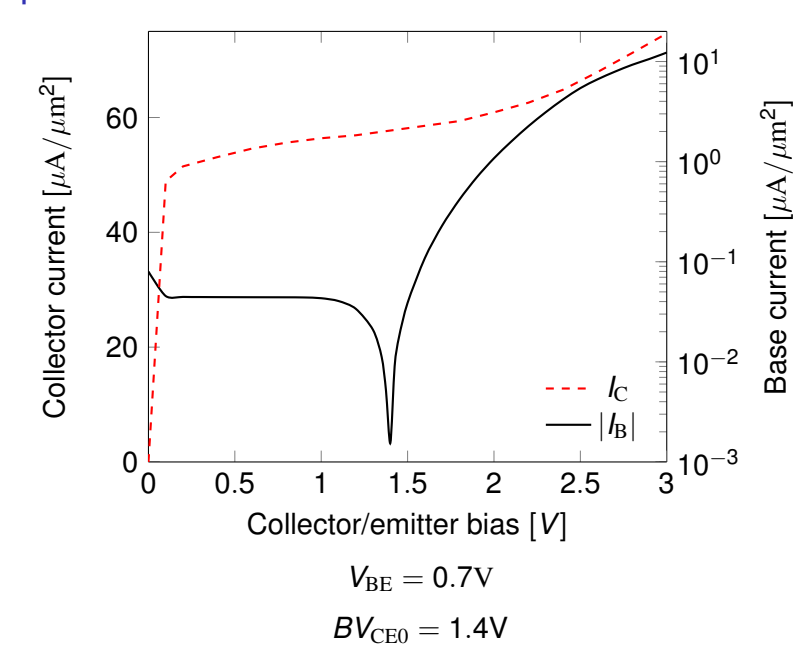
Emitter-window width: 2 × 25nm

- ▶ 149 nodes in x-direction
- ▶ 20 nodes in *y*-direction
- 5th order SHE expansion (21 spherical harmonics)
- ▶ Up to 1.42 · 10⁸ unknown variables (spacing in energy is 5.17meV and number of energy grid points depends on bias)
- Over 200 GB of memory required (for AC)
- ▶ Up to 10⁵ CPU-seconds for a DC point

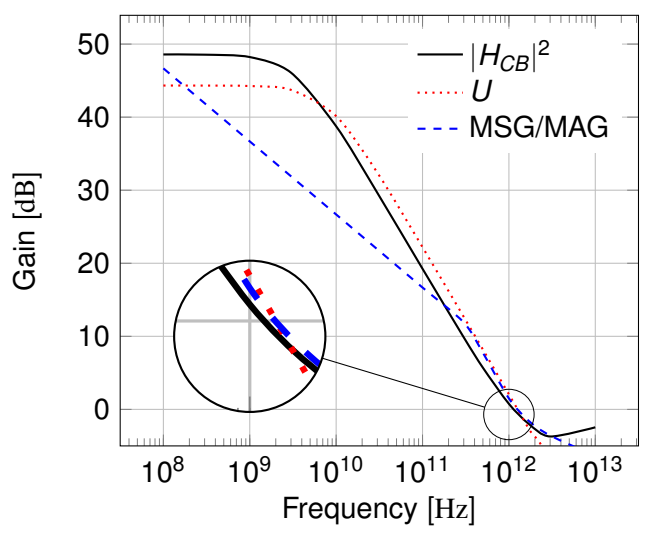


Base thickness: 7nm



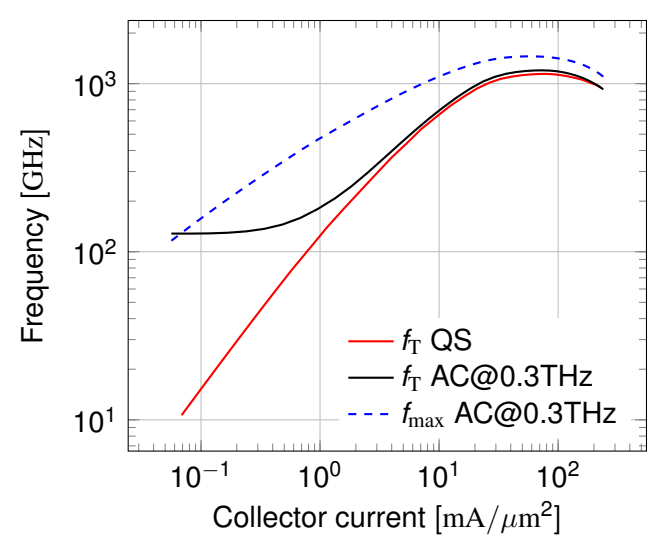


Gains



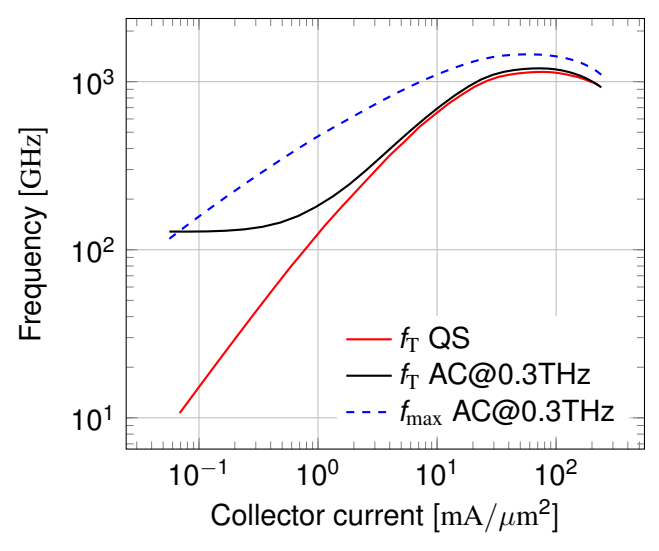
 $V_{BE} = 0.88 \text{V}, V_{CE} = 1.0 \text{V}, I_C = 18.2 \text{mA}/\mu\text{m}^2$

Cutoff and max. oscil. frequencies



 $V_{\rm CE}=$ 1.0V , $f_{
m max}$ by extrapolation of U peak $f_{
m T}=$ 1.2THz, peak $f_{
m max}=$ 1.45THz

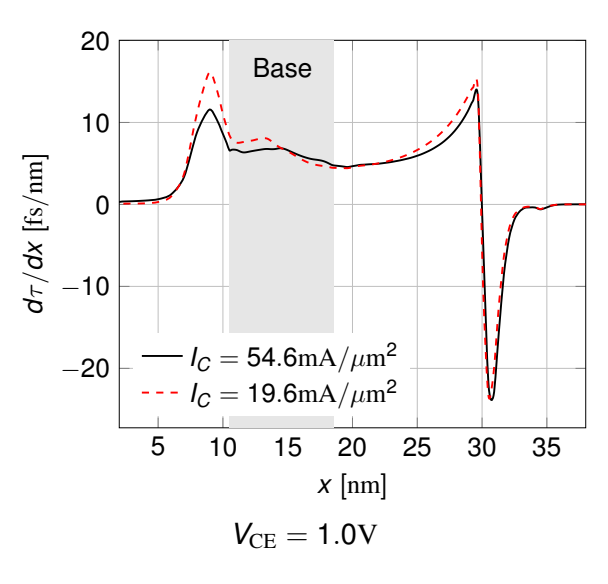
Cutoff and max. oscil. frequencies

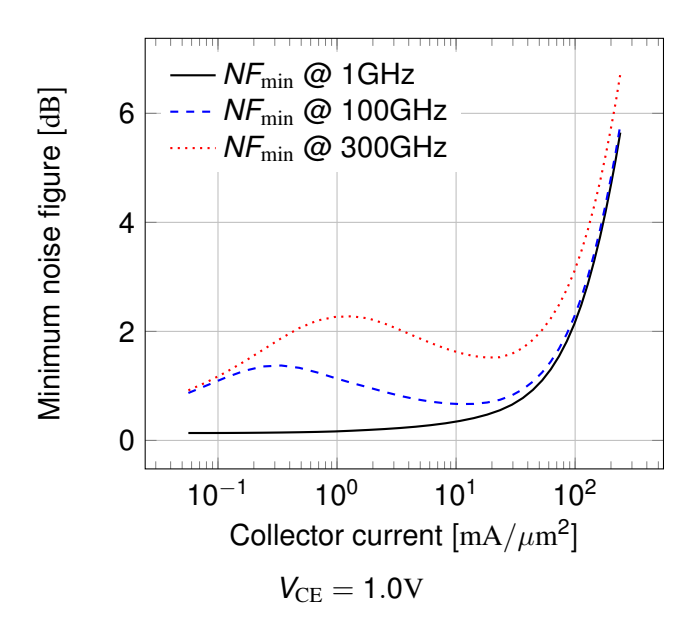


 $V_{\rm CE}=1.0{
m V}$, $f_{\rm max}$ by extrapolation of U peak $f_{\rm T}=1.2{
m THz}$, peak $f_{\rm max}=1.45{
m THz}$

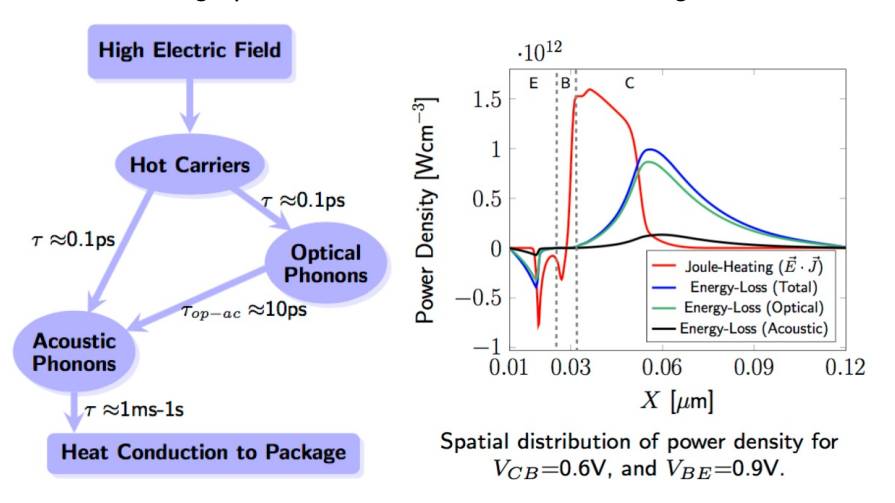
Local contribution to the transit time

$$f_{\mathrm{T}}=rac{1}{2\pi au}\;,\quad au=\intrac{d au}{dx}dx\;$$



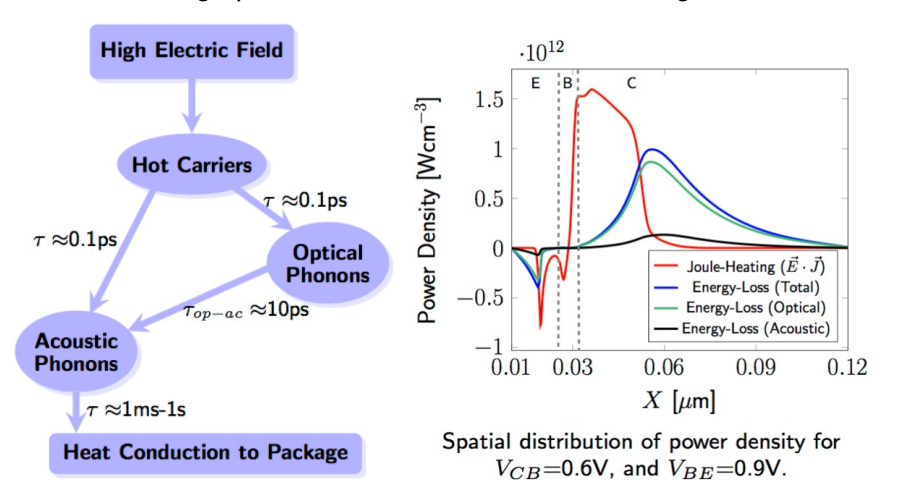


High power densities lead to self-heating

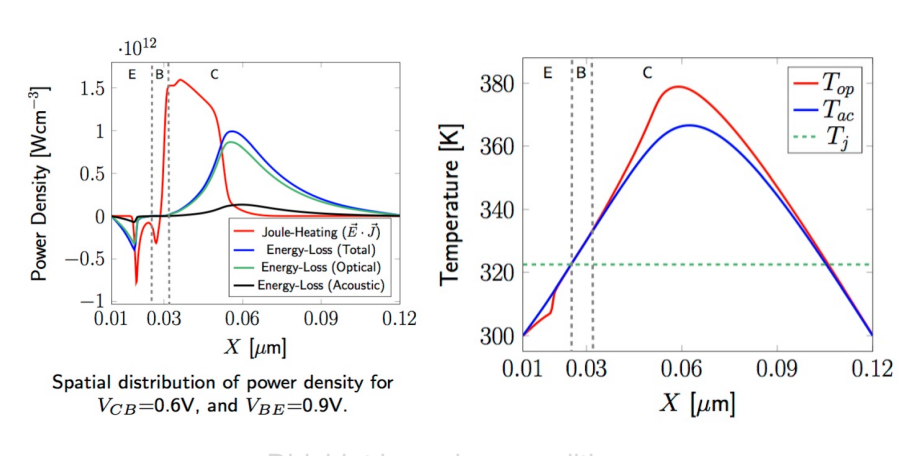


Heating is non-local!

High power densities lead to self-heating

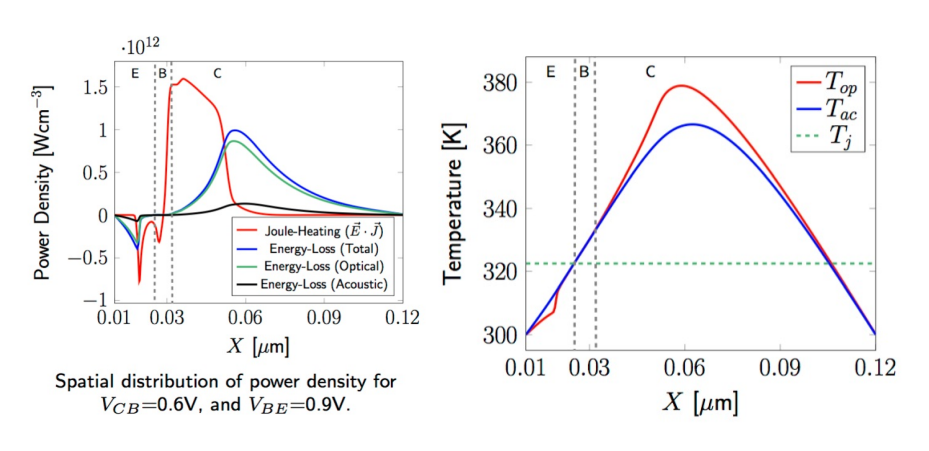


Heating is non-local!



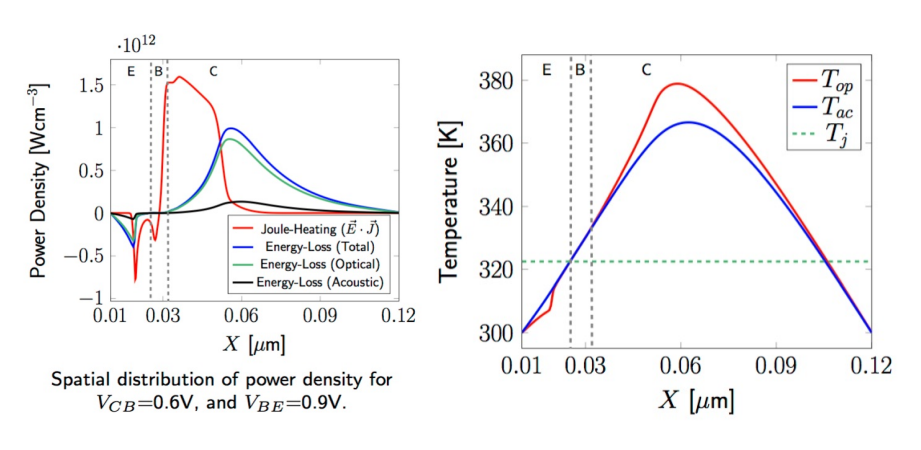
Dirichlet boundary conditions

Scattering between optical and acoustic phonons goes both ways



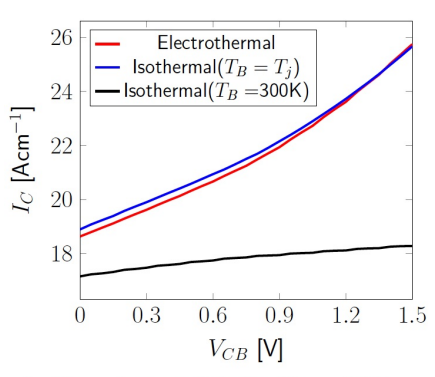
Dirichlet boundary conditions

Scattering between optical and acoustic phonons goes both ways

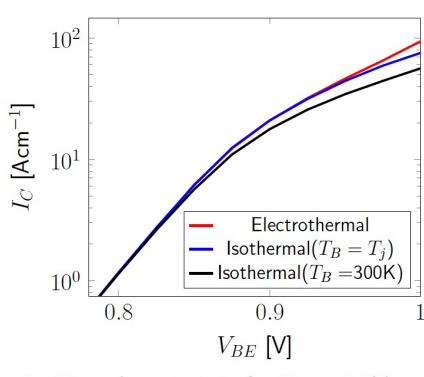


Dirichlet boundary conditions

Scattering between optical and acoustic phonons goes both ways

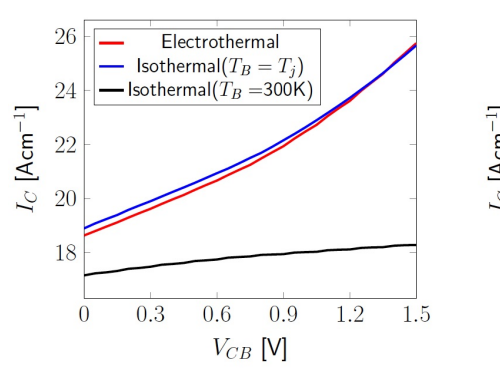


 $\it I_C\text{-}V_{CB}$ characteristic for $\it V_{BE}$ =0.9V.

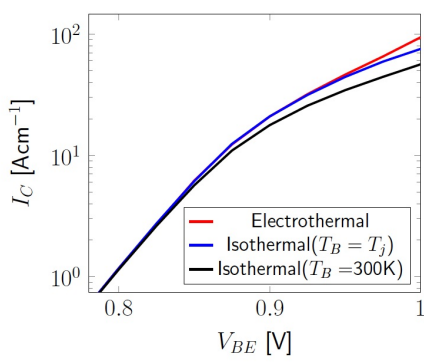


 I_C - V_{BE} characteristic for V_{CB} =0.6V.

Junction temperature determines the current Self-heating can lead to thermal runaway



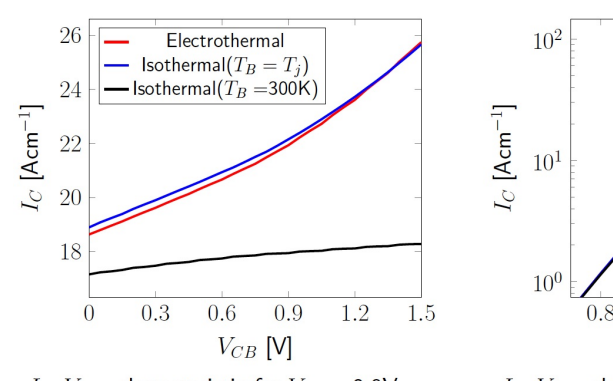
 I_C - V_{CB} characteristic for V_{BE} =0.9V.



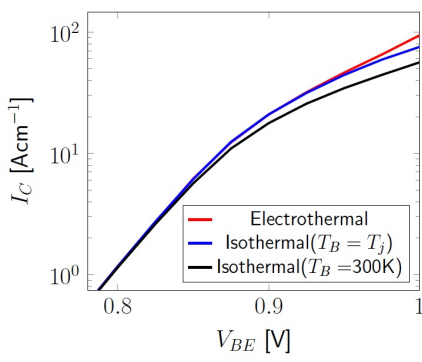
 I_C - V_{BE} characteristic for V_{CB} =0.6V.

Junction temperature determines the current

Self-heating can lead to thermal runaway



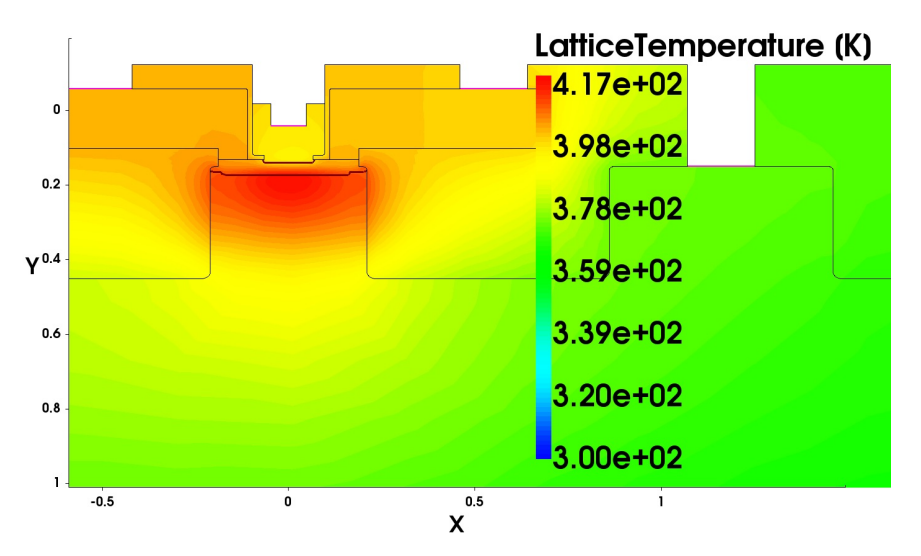
 $I_C\text{-}V_{CB}$ characteristic for V_{BE} =0.9V.



 I_C - V_{BE} characteristic for V_{CB} =0.6V.

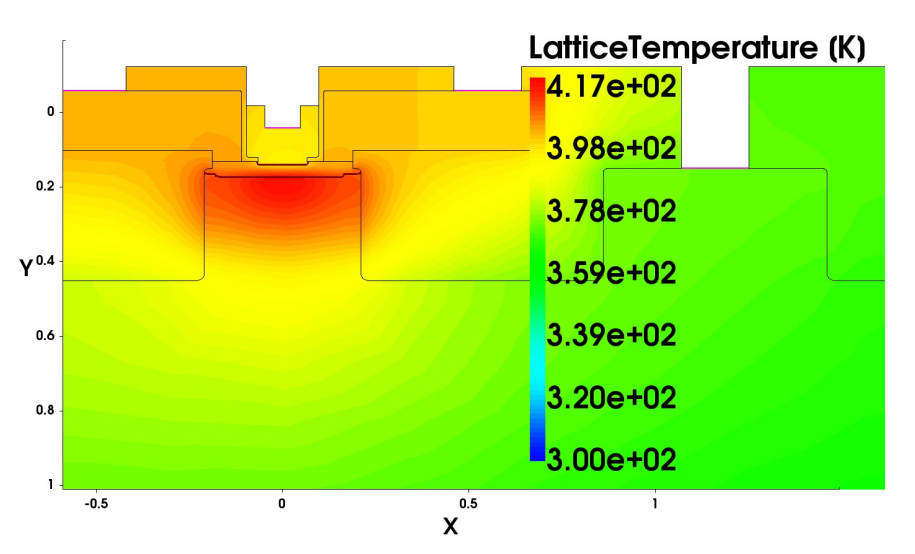
Junction temperature determines the current Self-heating can lead to thermal runaway

2D electrothermal simulation with SHE



Exact thermal simulation requires 3D simulation including metalization

2D electrothermal simulation with SHE



Exact thermal simulation requires 3D simulation including metalization

- Various effects can be included at a microscopic level
- DC, AC and noise analysis
- Device degradation, self-heating, mechanical strain, ...
- Transport at the nanoscale is very complex

- Various effects can be included at a microscopic level
- DC, AC and noise analysis
- Device degradation, self-heating, mechanical strain, ...
- Transport at the nanoscale is very complex

- Various effects can be included at a microscopic level
- DC, AC and noise analysis
- Device degradation, self-heating, mechanical strain, .
- Transport at the nanoscale is very complex

- Various effects can be included at a microscopic level
- DC, AC and noise analysis
- Device degradation, self-heating, mechanical strain, ...
- Transport at the nanoscale is very complex

- Various effects can be included at a microscopic level
- DC, AC and noise analysis
- Device degradation, self-heating, mechanical strain, ...
- Transport at the nanoscale is very complex

57

- Various effects can be included at a microscopic level
- DC, AC and noise analysis
- Device degradation, self-heating, mechanical strain, ...
- Transport at the nanoscale is very complex